

SIMULATION OF WATER EFFECT ON BIODIESEL PRODUCTION USING WASTE COOKING  
OIL VIA ESTER-TRANSESTERIFICATION IN A REACTIVE DISTILLATION COLUMN



A Thesis Submitted in Partial Fulfillment of the Requirements  
for the Degree of Master of Engineering in Chemical Engineering

Department of Chemical Engineering

Faculty of Engineering

Chulalongkorn University

Academic Year 2018

Copyright of Chulalongkorn University

การจำลองผลกระทบของน้ำต่อการผลิตไบโอดีเซลโดยใช้น้ำมันใช้แล้วผ่านปฏิกิริยาเอสเทอร์-  
ทรานส์เอสเทอร์ฟิเคชันในหอกั่นแบบมีปฏิกิริยา



วิทยานิพนธ์นี้เป็นส่วนหนึ่งของการศึกษาตามหลักสูตรปริญญาวิศวกรรมศาสตรมหาบัณฑิต  
สาขาวิชาวิศวกรรมเคมี ภาควิชาวิศวกรรมเคมี  
คณะวิศวกรรมศาสตร์ จุฬาลงกรณ์มหาวิทยาลัย  
ปีการศึกษา 2561  
ลิขสิทธิ์ของจุฬาลงกรณ์มหาวิทยาลัย



อจลา อนันต์พิณีพัฒนา : การจำลองผลกระทบของน้ำต่อการผลิตไบโอดีเซลโดยใช้  
น้ำมันใช้แล้วผ่านปฏิกิริยาเอสเทอร์-ทรานส์เอสเทอร์ฟิเคชันในหอกลั่นแบบมีปฏิกิริยา. (   
SIMULATION OF WATER EFFECT ON BIODIESEL PRODUCTION USING WASTE  
COOKING OIL VIA ESTER-TRANSESTERIFICATION IN A REACTIVE  
DISTILLATION COLUMN) อ.ที่ปรึกษาหลัก : ศ. ดร.สุทธิชัย อัสสะบำรุงรัตน์, อ.ที่  
ปรึกษาร่วม : ผศ. ดร.กนกวรรณ จ้าวสุวรรณ

งานวิจัยนี้ได้ศึกษาเกี่ยวกับผลกระทบของน้ำที่ปนเปื้อนในน้ำมันพืชใช้แล้วต่อสมรรถนะของ  
หอกลั่นแบบมีปฏิกิริยาสำหรับผลิตไบโอดีเซลผ่านปฏิกิริยาเอสเทอร์-ทรานส์เอสเทอร์ฟิเคชัน ไตรโอเลอิน  
ผสมกับกรดโอเลอิกถูกใช้เป็นสารประกอบจำลองของน้ำมันพืชใช้แล้ว สำหรับปฏิกิริยาเอสเทอร์ฟิเคชันจะ  
ใช้ตัวเร่งปฏิกิริยาแอมเบอร์ซิส-15 ในขณะที่ปฏิกิริยาทรานส์เอสเทอร์ฟิเคชันจะใช้แคลเซียมออกไซด์เป็น  
ตัวเร่งปฏิกิริยา จากการใช้แบบจำลองของแลงก์เมียร์-ฮินเชล์วูด-ออยล์เกน-วัตสันพบ (LHHW) ที่รวมการ  
ดูดซับของน้ำพบว่าผลได้ของไบโอดีเซลลดลงเมื่อน้ำมันพืชที่ใช้แล้ว (WCO) มีปริมาณน้ำเพิ่มขึ้น แต่ในทาง  
ตรงกันข้ามอัตราการเกิดปฏิกิริยาเริ่มต้นของปฏิกิริยาทรานส์เอสเทอร์ฟิเคชันจะเพิ่มขึ้นเมื่อน้ำมัน WCO  
มีปริมาณน้ำเพิ่มขึ้น 0-5%ต่อมวลน้ำมัน แต่อย่างไรก็ตามเมื่อผลได้ของไบโอดีเซลถึงค่าสูงสุดประมาณ  
30-40% และจะลดลงอย่างมีนัยสำคัญ เนื่องจากการเกิดปฏิกิริยาข้างเคียงหรือการเกิดสบู่ และเกิด  
อิมัลชันระหว่างสารตั้งต้นและผลิตภัณฑ์ ดังนั้นในควมมีการป้องกันไม่ให้มีน้ำในสารป้อน เพื่อป้องกันการ  
เกิดสบู่ แม้ว่าจะใช้ตัวเร่งปฏิกิริยาวิธพันธุแคลเซียมออกไซด์สำหรับการผลิตไบโอดีเซลก็ตาม เป็นที่  
น่าสนใจสำหรับหอกลั่นไฮบริดซ์แบบมีปฏิกิริยาสามารถรับสารป้อน มีน้ำปริมาณ 0-8%wt ซึ่งมีกพบ  
ทั่วไปใน WCO โดยพบว่าน้ำจะระเหยขึ้นสู่ด้านบนของหอโดยไม่ไหลลงมาในส่วนของปฏิกิริยาทรานส์เอ  
สเตอร์ฟิเคชัน โดยหอกลั่นไฮบริดซ์นี้สามารถผลิตไบโอดีเซลได้ผลได้ 97% และมีความบริสุทธิ์ 96.5 5 ซึ่ง  
ผ่านมาตรฐาน EN 14214 โดยใช้จำนวน 26 ชั้น อัตราการรีฟลักซ์ 0.1 และพลังงานในหม้อต้ม 50-128  
kW จากการป้อน WCO ด้วยอัตรา 1 kmol/h

สาขาวิชา วิศวกรรมเคมี  
ปีการศึกษา 2561

ลายมือชื่อนิสิต .....  
ลายมือชื่อ อ.ที่ปรึกษาหลัก .....  
ลายมือชื่อ อ.ที่ปรึกษาร่วม .....

# # 5970402321 : MAJOR CHEMICAL ENGINEERING

KEYWORD: Effect of water, Hybridized reactive distillation

Ajala Anantapinitwatna : SIMULATION OF WATER EFFECT ON BIODIESEL PRODUCTION USING WASTE COOKING OIL VIA ESTER-TRANSESTERIFICATION IN A REACTIVE DISTILLATION COLUMN. Advisor: Prof. Suttichai Assabumrungrat, Ph.D. Co-advisor: Asst. Prof. Kanokwan Ngaosuwan, D.Eng.

This research investigated the effect of water content in waste cooking oil (WCO) on the performance of a reactive distillation column for biodiesel production via ester-transesterification. A mixture of triolein and oleic acid was used as a WCO model compound. Amberlyst-15 was used to catalyze esterification while CaO was used for transesterification. From Langmuir-Hinshelwood-Hougen-Watson (LHHW) kinetic model taking into account water absorption for esterification of oleic acid (FFA), biodiesel yield was decreased with increasing of water content in WCO feedstocks. On the other hand, the initial rate of transesterification was increased with increase of amount of water in WCO feedstocks in the range of 0-5%wt. However, when biodiesel yield reached the maximum value of 30-40%, saponification as a side reaction became significant and the emulsion phase of feedstocks was present, resulting in significant decrease in biodiesel yield. Therefore, the water contaminated in feedstocks should be avoided because of the presence of saponification even when using heterogeneous CaO catalyst for biodiesel production. Interestingly, hybridized reactive distillation can handle the feedstocks with the presence of water in the range of 0-8%wt commonly found in most WCO sources. It was found that the water was vaporized to the top of the column and did not flow down to the transesterification section. The hybridized reactive distillation can produce 97% biodiesel yield with 96.5% biodiesel purity according to EN14214 standard with the use of total stages of 26, reflux ratio of 0.1 and reboiler duty of 50-128 kW for the WCO feed of 1 kmol/h

Field of Study: Chemical Engineering

Student's Signature .....

Academic Year: 2018

Advisor's Signature .....

Co-advisor's Signature .....

## ACKNOWLEDGEMENTS

I would like to express the deepest appreciation to my advisor, Professor Dr. Suttichai Assabumrungrat, for sharing expertise, and sincere and valuable guidance and encouragement extended to me. In addition, I wish to express my sincere thanks to Assistant Professor Dr. Kanokwan Ngaosuwan, my co-advisor, for her kind suggestions throughout my project and very patiently corrected my writing. I would grateful to thank to Associate Professor Dr. Kasidit Nootong as the chairman, Dr. Rungthiwa Methaapanon and Assistant Professor Dr. Worapon Kiatkittipong as the members of the thesis committee for their kind.

Moreover, I would like to acknowledge Assistant Professor Dr. Amata Anantpinijwatna, my brother, for he suggestion and program assistance. I appreciate my group MAP and all the staffs in Center of Excellence in Catalysis and Catalytic Reaction Engineering, Chulalongkorn University for their kind help and co-operation throughout my study period.

Finally, I would like to acknowledge to my beloved family, they are part of my success. They always support me in every way and give me many convenient things. I can say that I could not achieve my degree without their encouragements. Thank you so much.

จุฬาลงกรณ์มหาวิทยาลัย  
CHULALONGKORN UNIVERSITY

Ajala Anantapinitwatna

## TABLE OF CONTENTS

	Page
ABSTRACT (THAI).....	iii
ABSTRACT (ENGLISH).....	iv
ACKNOWLEDGEMENTS .....	v
TABLE OF CONTENTS .....	vi
TABLES CONTENT .....	ix
FIGURES CONTENT.....	x
Chapter 1 Introduction.....	1
1.1 Introduction.....	1
1.2 Objectives .....	4
1.3 Scope of works .....	4
1.4 Expected output.....	5
Chapter 2 Theory .....	6
2.1 Biodiesel production.....	6
2.2 Biodiesel feedstocks .....	6
2.3 Biodiesel production method.....	12
2.4 Reaction for biodiesel production .....	12
2.4.1 Transesterification.....	12
2.4.2 Esterification.....	13
2.4.3 Hydrolysis .....	13
2.4.4 Saponification .....	13
2.5 Catalyst.....	13

2.6 Biodiesel production conventional process .....	15
2.7 Biodiesel production reactive distillation process.....	17
2.8 Kinetic reaction and activation energy.....	19
2.8.1 Rate of reaction.....	19
2.8.2 Activation energy .....	21
Chapter 3 Literature review .....	22
3.1 Conventional and reactive distillation processes.....	22
3.2 Kinetic and mechanism of biodiesel reaction.....	27
3.2.1 Acid catalyst (Amberlyst-15) for esterification .....	27
3.2.2 Base catalyst (Calcium oxide, CaO) for transesterification .....	29
3.2.3 Base catalyzed saponification .....	31
Chapter 4 Kinetic experiment and simulation.....	33
4.1 Kinetics of esterification .....	33
4.1.1 Materials.....	33
4.1.2 Experimental.....	33
4.2 Kinetics of transesterification.....	33
4.2.1 Determination of the empirical rate model.....	34
4.2.2 Determination of activation energy (Ea).....	35
4.2.3 Materials.....	35
4.2.4 Experimental.....	35
4.3 Sample analysis .....	36
4.4 Simulation.....	36
Chapter 5 Results and discussion .....	37
5.1 Esterification .....	37



5.1.1 Kinetic model verification for esterification of oleic acid.....	37
5.1.2 Validation of esterification in RD.....	38
5.2 Transesterification .....	39
5.2.1 Determining the rate reaction of Transesterification in the presence of water .....	39
5.2.2 Determining the rate reaction of Transesterification in the absence of water .....	45
5.3 Reactive distillation: effect of design parameter.....	47
5.3.1 Hybridized RD in the presence of water for transesterification section....	49
5.3.2 Hybridized RD in absence of water in transesterification section.....	51
5.3.2.1 Water content in feed WCO.....	51
5.3.2.2 Number of stages .....	53
5.3.2.3 Methanol and oil feed location .....	55
Chapter 6 Conclusions and recommendation .....	59
REFERENCES .....	61
Appendix A Calibration curves for determining kinetic of esterification and transesterification.....	67
Standard curve of methyl oleate (FAME) .....	67
Standard curve of oleic acid.....	67
Appendix B Calculations of conversion and yield for esterification and transesterification.....	68
Esterification.....	68
Transesterification.....	68
Appendix C Verification of kinetic esterification.....	69

Appendix D Empirical kinetic model for transesterification of triolein in presence of water .....	70
Initial rate and overall rate .....	70
Polymath regression.....	72
MatLab code.....	76
Appendix E Empirical kinetic model for saponification.....	78
Polymath regression.....	78
Appendix F Empirical kinetic model for transesterification of triolein in absence of water .....	81
First order .....	81
Second order .....	82
Appendix G Hybridized RD in presence of water data .....	83
Appendix H Hybridized RD in absence of water data.....	85
VITA.....	89

## TABLES CONTENT

<b>Table 2.1</b> Feedstocks for biodiesel productions.....	7
<b>Table 2.2</b> The properties of different vegetable oils .....	7
<b>Table 2.3</b> Formula, molecular weight and properties of fatty acids and their methyl and ethyl esters. [เติม reference].....	9
<b>Table 2.4</b> ASTM D6751 (United States): Standard Specification for Biodiesel (B100) Blend Stock for Distillate Fuels.....	10
<b>Table 2.5</b> EN 14214 (Europe): Automotive Fuels: FAME for Diesel Engines. Requirements and Test Methods.....	11
<b>Table 3.1</b> Kinetic parameters for the modified LHHW model.....	28
<b>Table 4.1</b> Initial mole ratio and percent water of each run.....	34
<b>Table 5.1</b> Kinetic constants from CaO catalyzed transesterification .....	44
<b>Table 5.2</b> Kinetic model used for simulation of hybridized RD.....	48
<b>Table 5.3</b> WCO feedstocks and methanol composition .....	49

## FIGURES CONTENT

Figure 2.1 Heterogeneous catalytic reaction step .....	15
Figure 2.2 Process flow diagram of conventional homogeneous acid/base-catalyzed transesterification reaction.....	16
Figure 2.3 Flow sheet of ideal reactive distillation column .....	17
Figure 3.1 Conventional process for biodiesel production using heterogeneous catalyst.....	22
Figure 3.2 Biodiesel production process by reactive distillation column using heterogeneous catalyst.....	23
Figure 3.3 Liquid composition profiles within the reactive distillation column using heterogeneous catalyst.....	24
Figure 3.4 Schematic diagram of reactive distillation system.....	25
Figure 3.5 Hybridization in a single reactive distillation for biodiesel production .....	26
Figure 3.6 Results of two kinetic experiments with different initial amounts of water	28
Figure 3.7 Effect of water content of methanol on biodiesel yield. ....	30
Figure 3.8 The effect of water (a, left) and FFA content (b, right).....	30
Figure 3.9 Saponification of alkyl esters (a) reaction mechanism for alkyl esters saponification; (b) bimolecular collision by solvated hydroxide ions to form H-bond stabilized tetrahedral intermediate .....	32
Figure 5.1 Kinetic model fitted eq.3.3 (continuous line) and experiment (•).....	37
Figure 5.2 Acid conversion as a function of reflux ratio. Experimental data (•) [8] and simulation results (continuous line) .....	38
Figure 5.3 The effect of concentration of water on the initial transesterification rate	39
Figure 5.4 Results from experimental run 1-5, the concentration of FAME profile along the reaction time.....	40

Figure 5.5 Result of the concentration of FAME profile along the reaction time of experiment (▲1%wt, ■2%wt and ●5%wt of water content) and calculation from MatLab (··· 1%wt, - - 2%wt and — 5%wt of water content) .....	42
Figure 5.6 Result between ln rate and 1/T in Kelvin .....	43
Figure 5.7 Pseudo second-order reaction model of transesterification at various temperature 50-70°C.....	46
Figure 5.8 Result between ln rate and 1/T in Kelvin .....	46
Figure 5.9 Ester-transesterification in reactive distillation column.....	47
Figure 5.10 Liquid mass fraction in hybridized RD using TG with water content 5 %wt, methanol to TG molar ratio of 7:1, reflux ratio of 0.1 and residence time 5 min.....	50
Figure 5.11 Percent of water in liquid fraction in a hybridized RD using TG with water content 5 %wt, methanol to TG molar ratio of 7:1, reflux ratio of 0.1 and stage residence time of 5 min.....	50
Figure 5.12 Biodiesel yield and purity as function of residence time using methanol to TG molar ratio of 7:1 and reflux ratio of 0.1.....	51
Figure 5.13 Water mass fraction in reaction section different water content in feedstock 1-8 %wt.....	52
Figure 5.14 Biodiesel yield and purity as function of water content in WCO using methanol to TG molar ratio 7:1 and reflux ratio 0.1.....	52
Figure 5.15 Liquid mass fraction in a reactive distillation using TG with water content 5 %wt, methanol to TG molar ratio of 7:1 and reflux ratio of 0.1.....	54
Figure 5.16 Biodiesel yield and purity as function of number stage for transesterification using methanol to TG ratio 7:1, water content of 5%wt and reflux ratio 0.1.....	55
Figure 5.17 Co-feed WCO and MEOH at stage 2 .....	55
Figure 5.18 Co-feed WCO and MEOH at stage 6 .....	56
Figure 5.19 Co-feed WCO and MEOH at stage 13 .....	56

Figure 5.20 Feed WCO at stage 2 and MEOH at stage 6..... 57

Figure 5.21 Feed WCO at stage 2 and MEOH at stage 25 ..... 57



## Chapter 1

### Introduction

#### 1.1 Introduction

Nowadays, the energy requirement is increased continuously every year. Conversely, fossil fuel is decreased and global warming issue has become the main problem in the world. Therefore, human has developed clean and renewable energy such as hydro power, solar energy, geothermal energy and bio energy to replace petroleum based energy.

Biodiesel is one of the considerable bio energy. It can replace petro-diesel fuel because the properties of biodiesel are similar to petro-diesel. Moreover, biodiesel is clean, sustainable and biodegradable energy which can reduce CO<sub>2</sub> emission [1]. The major feedstock used to produce biodiesel are such as vegetable oil, animal fat and waste cooking oil (WCO). As we know, the main cost of biodiesel from feedstocks is more than 70% of the overall production cost [2]. Low cost raw material such as waste cooking oil (WCO) is required to reduce biodiesel production cost. The cost of WCO is 50% cheaper than palm oil, especially in Thailand. However, the drawback of using WCO as a biodiesel feedstocks is due to its typically high free fatty acid (FFA) content derived from hydrolysis of triglycerides during frying process and presence of water content. FFA content in WCO can react with base catalyst via saponification simultaneously transesterification which consumes the catalyst resulting in lower yield of biodiesel. To address this problem, several researchers have proposed a two-step process in which the WCO first undergoes using acid catalyzed esterification to lower the FFA content (less than 1%wt) following by base-catalyzed transesterification [2-4].

As mentioned before, both esterification and transesterification require the selection of suitable types of catalyst to provide higher yield under mild condition. Acid catalyst is used for esterification while base catalyst is preferred to catalyze transesterification. For the conventional method of biodiesel production, catalyst is normally used in homogeneous phase such as NaOH, KOH, and HCl. Nevertheless, it has disadvantage because of its large effluent disposal problems, loss of catalyst and

high equipment cost due to the corrosiveness [2, 5, 6]. There is another choice for biodiesel production using heterogeneous catalyst such as anion ion-exchange resin, CaO and MgO. The heterogeneous catalysis can overcome homogeneous catalysis by elimination of the washing section and reduction of huge amounts of waste water; easier disposal of spent solid catalyst, cheaper catalyst cost in term of reusability, and high purity of the end product resulting to simplify process and eliminate the entire sections from the process schemes [7].

Biodiesel production process can be separated into two main parts including of the reaction and separation parts. The combination of reaction and separation within one unit operation is called reactive distillation (RD). This unit is especially used for equilibrium limited reaction and also consecutive reaction. RD is a promising alternative process for chemical production due to its direct removal of the products or intermediates resulting in higher conversions and selectivity in comparison with the classical, sequential approach unit. The most important application for RD is for equilibrium limited reactions such as esterification, ester-hydrolysis reaction, transesterification, and etherification [8].

RD consists of reaction part in the middle of column and non-reaction parts are rectifying at top and stripping at bottom of column [9]. Interoperability between reaction and separation is happened at the same time. It makes process easy to continuously operate because when reaction is taking place, product flows down to bottom and some substrate (high volatility compound) moves to the top of the column. It can reduce excessive use of a reactant. Previous work from Boon-anuwat et al. [10], who studied homogeneous and heterogeneous processes of conventional and RD processes using soybean oil and methanol as reactants. The results showed that RD process with heterogeneous catalyst can eliminate the requirement of processing separation and purification at cost-effective column design and operating conditions. The optimum condition was 4:1 of methanol to oil molar ratio, reflux ratio of 0.1, reboiler heat duty of 70 kW and 6 reactive stages. This condition provided a biodiesel purity of 97%wt, biodiesel yield of 97.5%, and required energy of 153.0 kWh/ton of FAME (i.e., 139.2 kWh/ton of FAME with allocation to 98% purity



of glycerol byproduct). To reduce biodiesel production cost, the change of feedstock from virgin oil to WCO can overcome this problem as mentioned above. However, this required a pre-treatment step to reduce FFA via esterification as presented by Noshadi [11]. Fatty acid methyl esters (FAME or biodiesel) from waste cooking oil in a RD using a heteropolyacid,  $H_3PW_{12}O_{40} \cdot 6H_2O$  as a catalyst. The optimum conditions were determined to be 116.23 mol/h total feed flow, feed temperature of 29.9°C, 1.3 kW reboiler duty, and 67.9 methanol to oil ratio. The optimum FAME yield was 93.98%. However, this work used a large methanol to oil ratio (30:1-70:1) because transesterification using acid catalyst was 4,000 times slower reaction compared to base catalyst so this process needed high methanol to oil ratio. Then, Pérez-Cisneros et al. [12] developed the integrated heterogeneous two-step reactive distillation process for biodiesel production. The reactive distillation columns was used to carry out the esterification and transesterification reactions using heterogeneous method. This process can convert FFA (more than 1%wt) in the vegetable oil to fatty acid ester (or biodiesel) before feeding continuously to transesterification RD column. Recently, Petchsoongsakul et al. [13] developed the hybridization of ester- and transesterification for biodiesel production in a single RD column. This process used heterogeneous catalyst including of Amberlyst-15 and  $CaO/Al_2O_3$ . The optimum condition was 4:1 of methanol to oil molar feed ratio, 0.1 of reflux ratio and net energy 216 kWh/kmol biodiesel. However, this process used pseudo-homogeneous kinetic model for ester and transesterification which did not take into account the water effect. When the esterification takes place, it produces water as a by-product and water might have effect on the catalyst activity which should be accounted into kinetic rate model.

Actually, raw WCO has contaminated with water about 2-8%wt. Therefore, the effect of water should be considered in the kinetic rate model for studying the effect of water on the performance of the reactive distillation. The presence of water in feed stream has effect on the catalytic activity for both Amberlyst-15 and  $CaO$

catalyst. The water could have effect on the swelling and poisoning for amberlyst-15 [8]. While the presence of trace amount of water on CaO catalyst could generate more methoxide anions to promote transesterification rate and the biodiesel yield was improved within a short reaction time [14]. Steinigeweg and Gmehling [8] proposed the kinetic rate model of esterification of the fatty acid decanoic acid and methanol using a strong acidic ion-exchange resin (Amberlyst-15) as a catalyst. The sorption of water was account into this kinetic model using a Langmuir-Hinshelwood-Hougen-Watson (LHHW) approach. Therefore, this work aims to determine the empirical rate model accounting the concentration of water for transesterification using CaO as catalyst. Moreover, the simulation of the effect of water on the catalytic activity of esterification and transesterification using WCO where related to the design parameters of reactive distillation will be investigated.

## 1.2 Objectives

To simulate the effect of water in waste cooking oil on biodiesel production via ester-transesterification in a reactive distillation column

## 1.3 Scope of works

1. To verify kinetic model of Amberlyst-15 catalyzed esterification of decanoic acid in the presence of water using oleic acid.
2. To determine empirical rate model accounting the presence of water for CaO catalyzed transesterification in batch reactor using triolein as a model of triglyceride with various levels of water content in the range of 0 to 8%wt based on WCO in the temperature range of 50-70 °C.
3. To study the effect of water on the design parameter of reactive distillation (water contain in feedstock, number of stage and feed location) to obtain biodiesel yield and purity according to EN 14214 (FAME  $\geq$  96.5%)

#### 1.4 Expected output

To obtain accurate empirical kinetic model accounting the presence of water and to find suitable condition for producing biodiesel from waste cooking oil with trace amount of water in the reactive distillation.



## Chapter 2

### Theory

#### 2.1 Biodiesel production

Biodiesel can be used for diesel engines through 4 methods: blending with petrol-diesel, micro-emulsification (co-solvent blending), pyrolysis and transesterification [15]. First method is direct blending, vegetable oil mix with diesel directly but have many problems when used in diesel engine because property of biodiesel such as viscosity is high, acid value, FFA contaminant, and gum formation [16]. Second method is micro-emulsions, oil mix with methanol or ethanol and form emulsions. The problem is coke formation impact to incomplete combustion [16]. Third method is pyrolysis thermal cracking, it involves the catalytic transformation of the non-edible oils or animal fats in the absence of air or oxygen to liquid products having fuel properties similar to diesel. The pyrolysis material includes considerable amounts of sulfur, moisture, and sediments. The fourth method is transesterification and esterification, are the most common method to produce biodiesel because reactions operate at lower temperature than the pyrolysis. These reactions give product have properties closely petroleum diesel.

#### 2.2 Biodiesel feedstocks

Biodiesel can produce from variety of feedstocks as shown in Table 2.1. The main component of vegetable oils and animal fats are triglycerides including of three esters of fatty acid with one glycerol core. The triglycerides consist of difference fatty acid (FA) composition (Table 2.2), therefore their properties of physical and chemical are different. When FA react with methanol to produce fatty acid alkyl ester or biodiesel. It is fatty acid methyl ester and when react with ethanol call fatty acid ethyl ester as shows in Table 2.3.

Furthermore, biodiesel there are two commercial standards both American society for testing and material (ASTM D6751) and the European EN 14214 (Table 2.4, 2.5) [17].

**Table 2.1** Feedstocks for biodiesel productions [18]

Edible oils	Non-edible oil	Other sources
Cottonseed oil	Jatropha oil	Waste cooking oil
Coconut oil	Karanja (Pongamia oil)	Microalgae
Sunflower oil	Mahua oil	Animal fats
Canola oil	Neem	Beef tallow
Soybean oil	Linseed	Poultry fat
Castor oil	Polanga	Chicken fat
Mustard oil	Yellow oleander	Fish oil
Peanut oil	Rubber seed	Spirulina platensis algae
Palm oil	Eucalyptus oil	Chlorella protothecoides microalgae
Rapeseed oil		

**Table 2.2** The properties of different vegetable oils [19]

Type of Oil	Species	Fatty acid composition (%wt)	Viscosity (at 40 °C)	Density (g/cm <sup>3</sup> )	Flash point (°C)	Heating value (MJ/kg)	Acid value (mg KOH/g)	Cloud point (°C)	Pour point (°C)
Edible oil	Soybean	C16:0, C18:1, C18:2	32.9	0.91	254	39.6	0.2	-3.9	-12.2
	Rapeseed	C16:0, C18:0, C18:1, C18:2	35.1	0.91	246	39.7	2.92	3.9	-31.7
	Sunflower	C16:0, C18:0, C18:1, C18:2	32.6	0.92	274	39.6	-	18.3	-6.7
	Palm	C16:0, C18:0, C18:1, C18:2	39.6	0.92	267	-	0.1	31.0	-
	Peanut	C16:0, C18:0, C18:1, C18:2, C20:0, C22:0	22.72	0.90	271	39.8	3	12.8	-6.7
	Corn	C16:0, C18:0, C18:1, C18:2, C18:3	34.9	0.91	277	39.5	-	1.1	-40.0

Type of Oil	Species	Fatty acid composition (%wt)	Viscosity (at 40 °C)	Density (g/cm <sup>3</sup> )	Flash point (°C)	Heating value (MJ/kg)	Acid value (mg KOH/g)	Cloud point (°C)	Pour point (°C)
	Camelina	C16:0, C18:0, C18:1, C18:2, C18:3, C20:0, C20:1, C20:3	-	0.91	-	42.2	0.76	-	-
	Canola	C16:0, C18:0, C18:1, C18:2, C18:3	38.2	-	-	-	0.4	-	-
	Cotton	C16:0, C18:0, C18:1, C18:2	18.2	0.91	234	39.5	-	1.7	-5.0
	Pumpkin	C16:0, C18:0, C18:1, C18:2	35.6	0.92	>230	39	0.55	-	-
Non-edible	Jatropha curcas	C16:0, C16:1, C18:0, C18:1, C18:2	29.4	0.92	225	38.5	28	-	-
	Pongamina pinnata oil	C16:0, C18:0, C18:1, C18:2, C18:3	27.8	0.91	205	34	5.06	-	-
	Sea mango	C16:0, C18:0, C18:1, C18:2	29.6	0.92	-	40.86	0.24	-	-
	Palanga	C16:0, C18:0, C18:1, C18:2	72.0	0.90	221	39.25	44	-	-
	Tallow	C14:0, C16:0, C16:1, C17:0, C18:0, C18:1, C18:2	-	0.92	-	40.05	-	-	-
Others	WCO	Depends on fresh cooking oil	44.7	0.90	-	-	2.5	-	-
	Diesel		3.06	0.855	76	43.8	-	-	-16

**Table 2.3** Formula, molecular weight and properties of fatty acids and their methyl and ethyl esters.

Fatty acid Methyl ester Ethyl ester	Formula	Acronym*	Molecular weight (g/mol)	Higher heating value (MJ/kg)	Oxidation stability (h)	Kinematic viscosities (cSt)
Palmitic acid	$C_{16}H_{32}O_2$	$C_{16:0}$	256.40	-	-	-
Methyl palmitate	$C_{17}H_{34}O_2$		256.42	39.18	22.13	4.41
Ethyl palmitate			284.48	40.64	23.76	4.62
Stearic acid	$C_{18}H_{36}O_2$	$C_{18:0}$	284.48	-	-	-
Methyl stearate	$C_{19}H_{38}O_2$		298.51	40.21	17.93	5.82
Ethyl stearate			312.53	41.98	21.77	5.92
Oleic acid	$C_{18}H_{34}O_2$	$C_{18:1}$	282.47	-	-	-
Methyl oleate	$C_{19}H_{36}O_2$		282.46	40.13	6.61	4.55
Ethyl oleate			310.51	41.63	6.68	4.81
Linoleic acid	$C_{18}H_{32}O_2$	$C_{18:2}$	280.45	-	-	-
Methyl linoleate	$C_{19}H_{34}O_2$		280.45	40.06	4.37	3.69
Ethyl linoleate			308.5	40.86	5.02	4.28
Linolenic acid	$C_{18}H_{30}O_2$	$C_{18:3}$	278.44	-	-	-
Methyl linolenic	$C_{19}H_{32}O_2$		278.43	39.98	3.87	3.22
Ethyl linolenic			306.5	40.69	4.23	3.46

**Table 2.4** ASTM D6751 (United States): Standard Specification for Biodiesel (B100) Blend Stock for Distillate Fuels. [17]

Property	Test method	Limits	Unit
Flash point (closed cup)	D 93	130.0 min	°C
Water and sediment	D 2709	0.050 max	% volume
Kinematic viscosity, 40°C	D 445	1.9 – 6.0	mm <sup>2</sup> /s
Sulfated ash	D 874	0.020 max	% mass
Sulfur	D 5453	0.0015 max or 0.05 max <sup>a</sup>	% mass
Copper strip corrosion	D 130	No. 3 max	
Cetane number	D 613	47 min	
Cloud point	D 2500	Report	°C
Carbon residue (100% sample)	D 4530	0.050 max	% mass
Acid number	D 664	0.80 max	mg KOH/g
Free glycerin	D 6584	0.020 max	% mass
Total glycerin	D 6584	0.240 max	% mass
Phosphorus content	D 4951	0.001 max	% mass
Distillation temperature, atmospheric equivalent temperature, 90% recovered	D 1160	360 max	°C

<sup>a</sup>The limits are for Grade S15 and Grade S500 biodiesel, respectively. S15 and S500 refer to maximum sulfur specifications (ppm).



**Table 2.5** EN 14214 (Europe): Automotive Fuels: FAME for Diesel Engines. Requirements and Test Methods. [17]

Property	Test method	Limits		Unit
		min	max	
Ester content	EN 14103	96.5		% (m/m)
Density; 15°C	EN ISO 3675	860	900	kg/m <sup>3</sup>
Viscosity; 40°	EN ISO 12185			
	EN ISO 3104 ISO 3105	3.5	5.0	mm <sup>2</sup> /s
Flash point	EN ISO 3679	120		°C
Sulfur content	EN ISO 20846 EN ISO 20884		10.0	mg/kg
Carbon residue (10% dist. residue)	EN ISO 10370		0.30	% (m/m)
Cetane number	EN ISO 5165	51		
Sulfated ash	ISO 3987		0.02	% (m/m)
Water content	EN ISO 12937		500	mg/kg
Total contamination	EN 12662		24	mg/kg
Copper strip corrosion (3 h, 50°C)	EN ISO 2160	1		
Oxidative stability, 110°C	EN 14112	6.0		H
Acid value	EN 14104		0.50	mg KOH/g
Iodine value	EN 14111		120	g iodine/100 g
Linolenic acid content	EN 14103		12	% (m/m)
Content of FAME with ≥ 4 double bonds			1	% (m/m)
Methanol content	EN 14110		0.20	% (m/m)
Monoglyceride content	EN 14105		0.80	% (m/m)
Diglyceride content	EN 14105		0.20	% (m/m)
Triglyceride content	EN 14105		0.20	% (m/m)
Free glycerine	EN 14105		0.02	% (m/m)
	EN 14106			
Total glycerine	EN 14105		0.25	% (m/m)
Alkali metals (Na + K)	EN 14108		5.0	mg/kg
	EN 14109			
Earth alkali metals (Ca + Mg)	prEN 14538		5.0	mg/kg
Phosphorus content	EN 14107		10.0	mg/kg

## 2.3 Biodiesel production method

Biodiesel can be used for diesel engines through 4 methods: blending with petrol-diesel, micro-emulsification (co-solvent blending), pyrolysis and transesterification [15].

First method is direct blending, vegetable oil mix with diesel directly but have many problems when used in diesel engine because property of biodiesel such as viscosity is high, acid value, FFA contaminant, and gum formation [16]. Second method is micro-emulsions, oil mix with methanol or ethanol and form emulsions. The problem is coke formation impact to incomplete combustion [16]. Third method is pyrolysis thermal cracking, it involves the catalytic transformation of the non-edible oils or animal fats in the absence of air or oxygen to liquid products having fuel properties similar to diesel. The pyrolysis material includes considerable amounts of sulfur, moisture, and sediments. The fourth method is transesterification and esterification, are the most common method to produce biodiesel because reactions operate at lower temperature than the pyrolysis. These reactions give product have properties closely petroleum diesel.

## 2.4 Reaction for biodiesel production

### 2.4.1 Transesterification

Transesterification or alcoholysis is simple way to produce biodiesel. This is a catalytic reaction between triglycerides (TG) and alcohol (R'OH) to produce fatty acid alkyl ester (Biodiesel, R'COOR) and glycerol as by product. Transesterification consists of three reversible reactions which are triglycerides converted to diglycerides (DG) then, diglycerides converted to monoglycerides (MG) followed by conversion of monoglycerides to glycerol (Eqs 2.1-2.3). Biodiesel is produced in each reaction. Therefore, the overall reaction for one molecule triglycerides should obtain 3 molecules of biodiesel as shown in Eq 2.4





#### Overall reaction



#### **2.4.2 Esterification**

Conversion of carboxylic acids to esters using acid and alcohols is shown in Eq 2.5. Mostly of esterification is used as pretreatment of oil when it has high free fatty acid (FFA,  $R'COOH$ ) content such as waste cooking oil. This reaction can produce water as a by-product. A side reaction is hydrolysis of triglyceride.



#### **2.4.3 Hydrolysis**

Triglycerides can be hydrolyzed to produce 1 molecule of glycerol and 3 molecules of FFAs in the presence of acid and heat or with a suitable lipase enzyme under biological conditions, namely hydrolysis. However, the product as FFAs can continued convert to biodiesel via esterification (Eq 2.6).



#### **2.4.4 Saponification**

Saponification can convert FFA to soap in either a one- or a two-step process. The FFA is treated with a strong base (e.g. NaOH, KOH shown in Eqs 2.7 and 2.8), which split the ester bond, releasing fatty acid salts (soaps) and glycerol. In some soap-making, the glycerol is left in the soap.



### **2.5 Catalyst**

Reaction rate can be accelerated by catalyst and activation energy can be decreased when using catalyst. The catalysts used for the ester-transesterification are mainly divided into two types including of homogeneous and heterogeneous

catalysts. However, the main problem of homogeneous is difficulty in catalysts extraction [19] and requires a tremendous amount of water for separation which have an impact to the environment [20]. Heterogeneous can use to overcome this problem. Acid catalyst is used for esterification such as tungsten oxide, zirconia, zeolites and heteropolyacids (Amberlyst-15) [21], transesterification can use both acid or base catalyst but base catalyst is faster than acid catalyst around 4,000 times. Therefore, base catalyst such as CaO [22], Mg-Zr [23], Zeolite [24], KI/Al<sub>2</sub>O<sub>3</sub> [25] and CaO/Al<sub>2</sub>O<sub>3</sub> [26] are used for transesterification.

The mechanism of heterogeneous catalyst reaction is controlled by catalytic reaction which can be explained step by step as follows [27]:

1. Diffusion mass transfer of the reactants from the bulk fluid to catalyst surface.
2. Diffusion of the reactant from the pore mouth through the catalyst pores to the immediate vicinity of the internal catalytic surface.
3. Adsorption of reactants onto the catalyst surface.
4. Reaction on the surface of the catalyst.
5. Desorption of the products from the catalyst surface.
6. Diffusion of the products from the interior of the pellet to the pore mouth at the external surface.
7. Mass transfer of the products from the external pellet surface to the bulk fluid.

The overall process by which heterogeneous catalytic reactions is shown in Figure 2.1

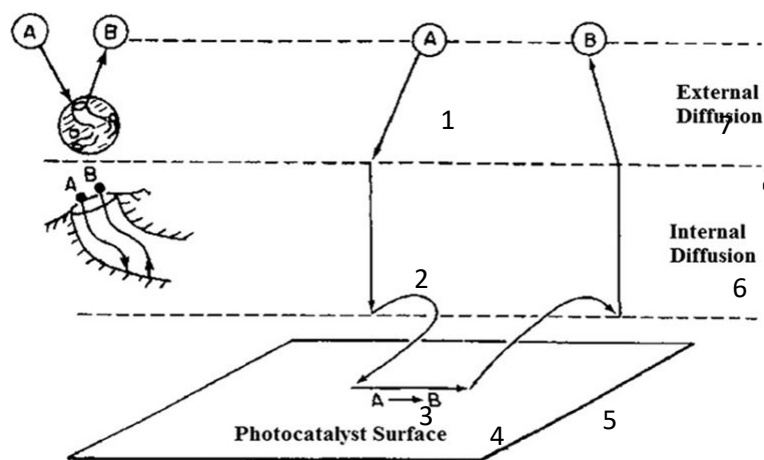


Figure 2.1 Heterogeneous catalytic reaction step [27]

The overall rate of reaction is equal to the rate of the slowest step in the mechanism. When compare step 1, 2, 6 and 7 of the diffusion steps faster than steps 3, 4 and 5 of the reaction step. Therefore, the rate of reaction of heterogeneous catalyst is a majority of the reaction step.

## 2.6 Biodiesel production conventional process

Conventional process for biodiesel production composes of several steps as shown in Figure 2.2. The process flow diagram of conventional homogeneous acid/alkaline-catalyzed transesterification. First step, homogeneous catalyst is mixed with alcohol then feed oil for react transesterification. After that, the reaction is need to neutralization for remove catalyst leftover in reaction mixture. Next step is separation to separate the polar and non-polar in decanter. The non-polar phase is biodiesel containing of a few methanol which required water for washing before sent to product tank and needed to dry under vacuum. Another phase is polar phase including of methanol and glycerol which re-neutralized because some catalyst dissolve in polar phase using the opposite chemical property. After that, this mixture is sent to distillation column to separate recycle methanol and glycerol as

byproduct. The glycerol will be purified to be valuable subtract for other process such as pharmaceutical process.

The conventional biodiesel production process have many problems. The main problem is the huge amount of waste water in washing step and at the neutralization used more chemical substance. However, there are many techniques and technologies to solve this problem. First techniques is used heterogenous catalyst to avoid washing step and neutralization because heterogenous catalyst can reused by regeneration. On the other hand, reactive distillation can choose to reduce unit operation for this fix problem because the configuration of reactive distillation combines reaction and distillation in single unit.

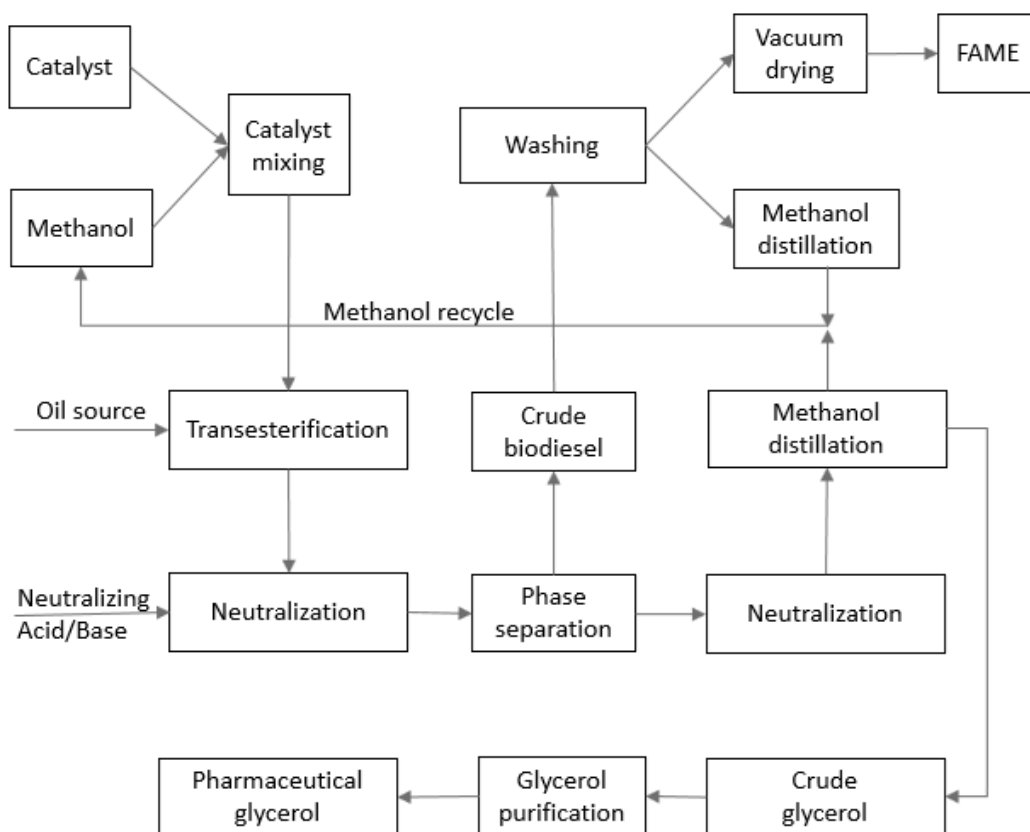


**Figure 2.2** Process flow diagram of conventional homogeneous acid/base-catalyzed transesterification reaction [28].

## 2.7 Biodiesel production reactive distillation process

As mentioned the conventional problem above, the intensification technology for biodiesel production is reactive distillation. The reactive distillation can solve many problems in biodiesel production such as to avoid the washing step, to reduce waste water and no catalyst neutralization step. The investment costs is reduced because of about 45% energy savings as compared to conventional biodiesel production. Moreover, reactive distillation provide the higher conversion, increase unit productivity and reduce the requirement of alcohol excess.

Reactive distillation consists of three parts: first is reaction part where in the middle of column and two non-reaction part are rectifying at top and stripping at bottom of column [9] as shown in Figure 2.3. Interoperability between reaction and separation is occurred at the same time. It makes process easy to continuous operate because when reaction is occurred, product is flow down to bottom and some substrate (high volatility compound) go to top the column. The main purpose of reactive distillation column is continuous removal of product from reactive zone to improve the conversion and shift equilibrium restrictions [29].

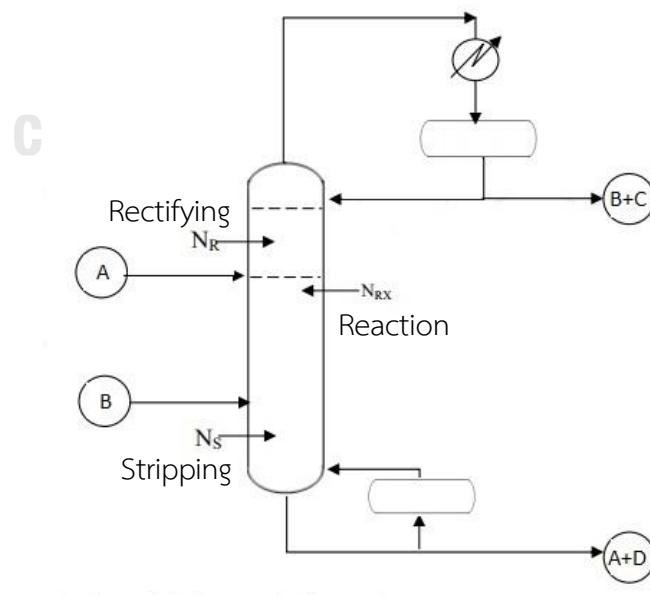


**Figure 2.3** Flow sheet of ideal reactive distillation column [29].

The basics concept of reactive distillation as thought the system of two precursor (A and B) producing two products (C and D). The reaction takes place in the liquid phase and is reversible (Eq 2.10).



For reactive distillation concept, we should be able to remove the products from the precursor by distillation of volatile product. For this reason, the products should be lighter or heavier than the precursors. In terms of the relative volatilities of the four components, an ideal case is when one component is the lightest and the other components is the heaviest, with the reactants being the intermediate boiling components (Eq 2.11).

$$\alpha_D > \alpha_C > \alpha_B \quad (2.11)$$

From the idea case can improve the reaction yield and conversion. Because in reactive distillation unit is a continuous separation of one product out of the reaction zone [9].

Figure 2.3 shows the flow sheet of this ideal reactive distillation column. Feed comprise of the heavier precursor A and lighter precursor B at upper and lower section of the column, respectively. The middle of the column is the reactive section and contains number of reaction trays ( $N_{RX}$ ). As precursor B flows up the column, it reacts with precursor A. The lighter product C is removed in the vapor phase and the heavier product D is also removed in the liquid phase from the reaction zone.

The section of the column above feed stage of A is rectifying section ( $N_R$ ) is used to separate the lighter product C from all of the heavier components. The section of the column below feed stage of B is stripping section ( $N_S$ ) is used to separate heavy product D from all of the lighter components resulting to fairly pure product D as a bottom product.



Temperature profile along the column is an important parameter for reactive distillation design because it affects the phase equilibrium and chemical kinetics. At the low temperature will slow the reaction rate which can be designed to increase liquid holdup (or increase amount of catalyst) in order to obtain a higher conversion. On the other hand, if high temperature operation will cause high reaction rate, which will result in the separation is done so rarely. For the above reasons, reactive distillation column should be considered in designing the appropriate operated with optimum temperature. Furthermore, there are other operating and design parameter should be considered including of number of stage (stripping, reactive, rectifying), feed locations, reflux ratio and reboiler heat duty.

## **2.8 Kinetic reaction and activation energy**

Chemical kinetics, also known as reaction kinetics, is the study of rates of chemical conversion or production. Chemical kinetics includes investigations of how different experimental conditions can influence the speed of a chemical reaction and product yield information on the reaction's mechanism, as well as the construction of mathematical models to describe the characteristics of a chemical reaction.

### **2.8.1 Rate of reaction**

Chemical kinetics deals with the experimental result to determine of reaction rates from which rate laws and rate constant are derived. For example, the simple rate laws exist for zero order reaction (for which reaction rates are independent of concentration), first order reaction, and second order reaction, and can be derived for others. In consecutive reaction, the rate-determining step often determines the overall kinetics rate, Moreover, a steady state approximation can also use to simplify the rate law for the consecutive first order reactions. The activation energy for a reaction is experimentally determined through the Arrhenius equation. The main factors that influence the reaction rate include: the physical state of the reactants, the concentration of the reactants, the temperature at which the reaction occurs, and whether or not any catalysts are present in the reaction[30].

The rate law or rate equation for a chemical reaction is an equation which links the reaction rate with concentrations or pressures of reactants and constant parameter. To determine the rate equation for a particle system one combines the reaction rate with a mass balance for the system.



For a generic reaction (Eq 2.12) the simple rate equation (as opposed to the much more common complicated rate equation) is of the form (Eq 2.13).

$$r = k(T)[A]^x[B]^y \quad (2.13)$$

This Eq 2.13. expresses the given reactant concentration, usually in mol/L (molarity). The  $k(T)$  is the reaction constant, although it is not really a constant because it includes everything that effects reaction rate outside concentration such as temperature but also including ionic strength, surface area of the adsorbent or light irradiation. The exponents  $x$  and  $y$  are the reaction orders and depended on the reaction mechanism. The stoichiometric coefficients and the reaction order are very often equal, but only in one step reactions molecularity (number of molecules or atoms actually colliding), stoichiometry and reaction order must be the same. The rate equation is a differential equation, and it can be integrated in order to obtain an integrated rate equation that corresponded to the concentrations of reactant or products with time. If the concentration of one of the reactants remains constant (because it is a catalyst or it is in large excess with respect to the other reactants) its concentration can be included in the rate constant, obtaining a pseudo constant: if B is the reactant whose concentration is constant then  $r=k[A][B]=k'[A]$ . This can make the treatment to obtain an integrated rate equation much easier.

### 2.8.2 Activation energy

For many reactions the rate expression can be written as a product of temperature dependent term and a composition dependent term (Eqs 14-15).

$$r_i = f_1(\text{temperature}) \cdot f_2(\text{composition}) \quad (2.14)$$

$$r_i = k \cdot f_2(\text{composition}) \quad (2.15)$$

For such reactions the temperature dependent term, the reaction rate constant has been found in practically all cases to be well represent by Arrhenius' law in Eq 2.16.

$$k = k_0 e^{\frac{-E_a}{RT}} \quad (2.16)$$

To rearrange the Arrhenius equation (Eq 2.17).

$$\ln k = \ln k_0 - \frac{E_a}{RT} \quad (2.17)$$

Where  $k_0$  is called the frequency or pre-exponential factor,  $E_a$  is the activation energy of the reaction (kJ),  $R$  is gas constant (8.314 kJ/(mol-K)) and  $T$  is temperature (K). This expression should fit experimental data well over wide temperature ranges and is strongly suggested from various standpoints as being a very good approximation to the true temperature dependency. From equation, a plot of  $\ln k$  vs  $1/T$  give a straight line, with a slope equal to  $E_a/R$ . Reactions with high activation energies are very temperature sensitive; reactions with low activation energies are relatively temperature insensitive.

## Chapter 3

### Literature review

#### 3.1 Conventional and reactive distillation processes

For conventional process, homogeneous catalyst for biodiesel production in chapter 2 have some drawbacks, therefore, in this chapter will focus on heterogeneous process.

The conventional biodiesel production from fresh vegetable oil or triglyceride was proposed by Boon-anuwat et al. [10] as shown in Figure 3.1. Feed stream of triglyceride and methanol were fed to the CSTR reactor where operated isothermally at 1 atm. The product stream containing biodiesel, glycerol and unreacted methanol were sent to a distillation column to remove unreacted methanol. Optimal condition was used methanol to triglyceride feed ratio of 15, reaction temperature of 70°C in terms of product purity. It was found that the necessity of using high methanol feed ratio and vacuum distillation, very high energy consumption of 754.8 kWh/ton FAME (with allocation to glycerol) were required. Glycerol purity from the decanter could meet the crude glycerol purity (>85%); hence the distillation column to obtain high purity grade glycerol was only optional.

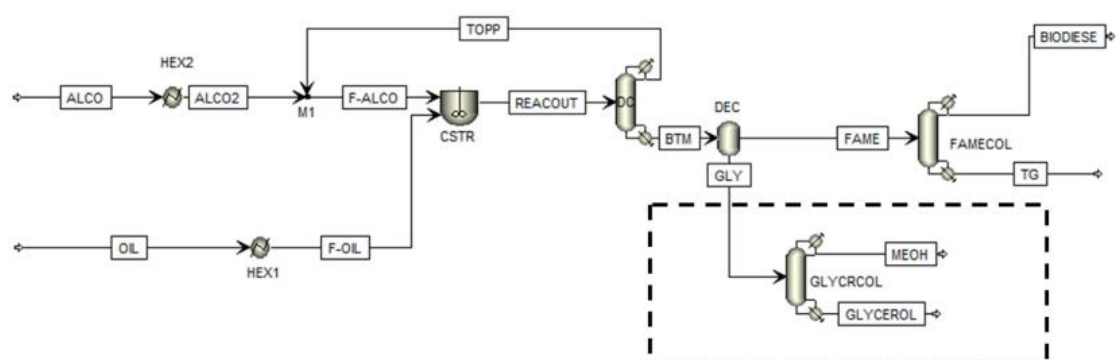


**Figure 3.1** Conventional process for biodiesel production using heterogeneous catalyst (dashed line represent optional distillation column to obtain technical grade glycerol) [10]

Reactive distillation was used to produce biodiesel as shown in Figure 3.2. At the top of RD feed triglyceride ( $60^{\circ}\text{C}$ ) while methanol was fed as vapor at the bottom of RD. The reactive distillation column was operated at a pressure of 1 bar, reflux ratio 0.1, bottom rate  $4.3\text{ kmol/h}$  and total 15 theoretical stages, consisting of no rectifying stage, 11 reaction stages and 2 stripping stages including of the condenser and the reboiler. Then, the bottom stream was sent to a decanter for high purity biodiesel recovery. Figure 3.3 shows the liquid composition profiles within the reactive distillation column. It can be seen that the top stream is methanol and bottom stream consists of biodiesel and glycerol. The temperature profile in the reactive distillation column was in the range of  $60$  to  $150^{\circ}\text{C}$ .

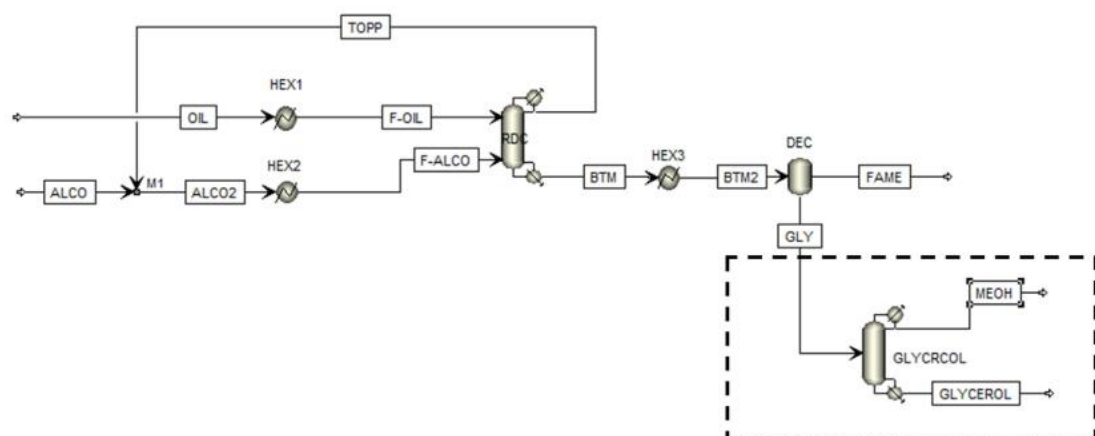


**Figure 3.2** Biodiesel production process by reactive distillation column using heterogeneous catalyst (dashed line represent optional distillation column to obtain technical grade glycerol) [10]

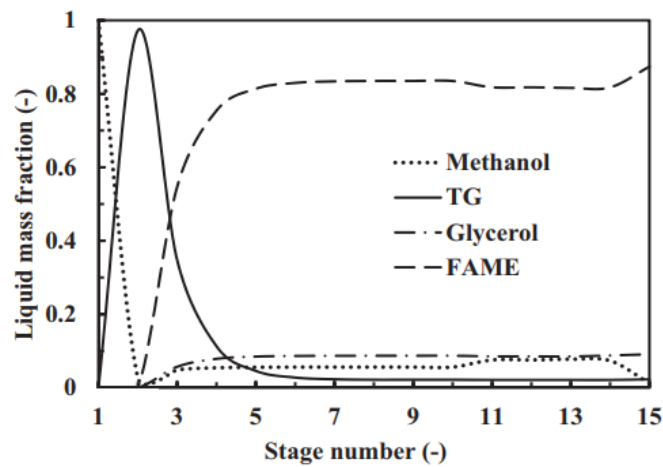


**Figure 3.3** Liquid composition profiles within the reactive distillation column using heterogeneous catalyst [10]

This process can reduce methanol to oil molar ratio from 15:1 to 4:1 and reduce unit operation when the reactive distillation combined reaction and distillation in one unit was used.

Although fresh oils was usually being as feedstocks for biodiesel production, the use of edible vegetable oils make the ‘food versus fuel’ debate on the use of large farmland areas for biofuel production influence of food supply [31]. Therefore, many researches [2, 21, 29, 32] proposed to use WCO as a feedstock. However, WCO might be contaminate with FFA and water which requires the washing step to reduce moisture and esterification step to reduce FFA before transesterification.

Noshadi et al. [11] studied biodiesel production using WCO and heterogeneous process in reactive distillation pilots scale (8 trays and inner diameter of 80 mm) as shown in Figure 3.4. WCO is needed to pre-heater at 50°C before feed to RD and then mixed with methanol with the presence of 12-Tungstophosphoric acid (10%wt with respect to WCO). Mechanical stirrer was used with speed of 300 rpm to form one liquid phase. Residence time in this mixer was depended on the feed flowrate with less than 60 min.

The optimal conditions of feed flow rate 116.23 mol/h, feed temperature 29.94°C, methanol/oil ratio 67.3 and reboiler duty 1.3 kW can produce the purity and actual FAME yield up to 93.98 and 93.94%, respectively.

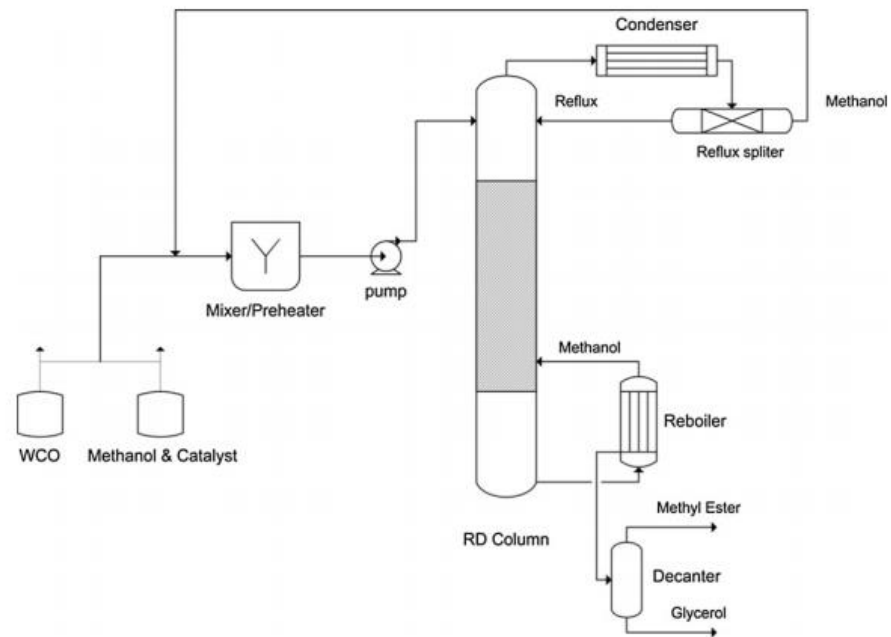


**Figure 3.4** Schematic diagram of reactive distillation system [11]

This process required highly methanol/oil ratio because the acid catalyst was used for both esterification and transesterification. Reaction rate of acid catalyzed transesterification is very slow thus the highly methanol to oil ratio was used to accelerate reaction rate.

Petchsoongsakul et al. [13] designed the biodiesel production from waste cooking oil in a single reactive distillation scheme shown in Figure 3.5.

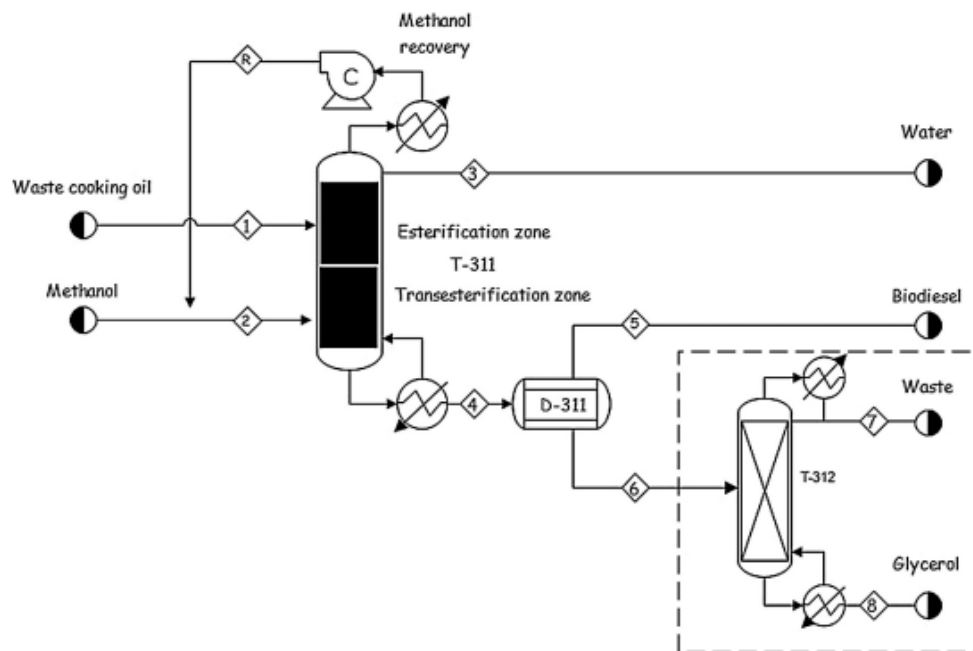


**Figure 3.5** Hybridization in a single reactive distillation for biodiesel production (dashed frame represents optional distillation column to obtain technical grade glycerol) [13]

This process combined esterification and transesterification in a single RD and operated at high pressure of 3 bar. The hybrid RD was divided into two parts including of the upper part for esterification and lower for transesterification using WCO with FFA content about 6%wt as a feedstock. FFA must be reduced below 1%wt before sent to transesterification. Methanol and WCO were fed at the second stage. In order to produce biodiesel according to standard, the suitable RD to produce biodiesel by hybridized RD using Amberlyst-15 and  $\text{CaO}/\text{Al}_2\text{O}_3$  catalyst include 4 stages for the esterification and 20 stages for the transesterification at atmospheric pressure. The optimum condition was found to be 4:1 of methanol to oil mol feed ratio, reflux ratio of 0.1 and reboiler heat duty of 216 kWh/kmol biodiesel. The bottom stream was sent to separate biodiesel from glycerol.

The pseudo-homogeneous kinetic model above which related to homogeneous catalyst has been used for all of simulation process. For



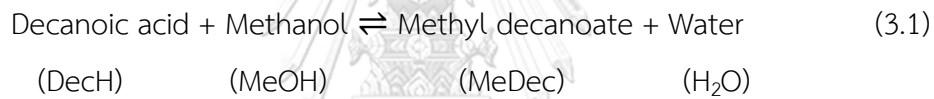
heterogeneous catalyst, the adsorption and desorption processes should be concerned.

### 3.2 Kinetic and mechanism of biodiesel reaction

#### 3.2.1 Acid catalyst (Amberlyst-15) for esterification

Steinigeweg and Gmehling [8] proposed a reactive distillation process for the production of decanoic acid methyl esters via esterification of the fatty acid decanoic acid and methanol as presented in Eq 3.1. A strong acidic ion-exchange resin (Amberlyst-15) has been used to catalyze esterification.

A pragmatic kinetic model based on a Langmuir-Hinshelwood-Hougen-Watson approach has been derived in Eq 3.2. Langmuir-Hinshelwood-Hougen-Watson (LHHW) approach is use to simplify the reaction rate with accounting for the sorption of water.



$$r = \frac{1}{v_i} \frac{dn_i}{dt} = m_{cat} \times \left( \frac{k_1^* K_{DecH} a_{DecH} K_{MeOH} a_{MeOH} - k_{-1}^* K_{MeDec} a_{MeDec} K_{H_2O} a_{H_2O}}{1 + (K_{DecH} a_{DecH} + K_{MeOH} a_{MeOH} + K_{MeDec} a_{MeDec} + K_{H_2O} a_{H_2O})} \right) \quad (3.2)$$

Water is adsorbed and therefore sorption effects can be summarized with a singular sorption constant  $K_{Sorb}$  as corresponding to Rehfinger and Hoffmann [33] who derived an equation for the synthesis of methyl tert-butyl ether using this simplification. Their approach can also be applied for an esterification. This leads to the following Eq 3.3.

$$r = \frac{1}{v_i} \frac{dn_i}{dt} = m_{cat} \left( \frac{k_1 a_{DecH} a_{MeOH}}{(k_{Sorb} a_{H_2O})^2} - \frac{k_{-1} a_{MeDec}}{k_{Sorb} a_{H_2O}} \right) \quad (3.3)$$

Then adjust five parameters ( $k_1^0$ ,  $k_{-1}^0$ ,  $E_{A,1}$ ,  $E_{A,-1}$ ,  $K_{\text{Sorb}}$ ) have to be fitted. The results are given in Table 3.1. This following equation can determine the influence of water on the reaction rate quantitatively. For fitting the sorption constant  $K_{\text{Sorb}}$  nine kinetic experiments have been performed under the conditions (i.e., initial amount of acid and alcohol, temperature, and amount of catalyst) for different amounts of water initially present. Figure 3.6 shows the weight fraction of decanoic acid as a function of time for two of these kinetic experiments. It can be seen that the adsorption-based model is able to describe the reaction rate for different water concentrations.

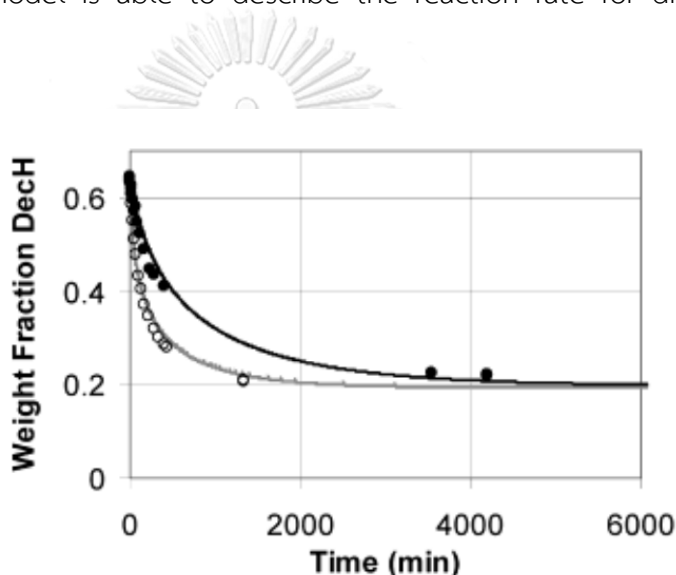


**Figure 3.6** Results of two kinetic experiments with different initial amounts of water. ( $T = 333 \text{ K}$ ,  $x_{\text{H}_2\text{O}}^0 = 0.019$ : (O) exp, (—) fitted Eq 3.3 ;  $x_{\text{H}_2\text{O}}^0 = 0.179$ : (•) exp, (—) fitted Eq 3.3). [8]

**Table 3.1** Kinetic parameters for the modified LHHW model Eq 3.2 ( $K_{\text{Sorb}} = 2.766$ ) [8]

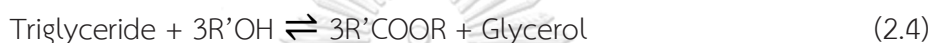
Reaction	$i$	$k_i^0$ (mol/ g s)	$E_{A,i}$ (kJ/mol)
Esterification	1	$3.1819 \times 10^6$	72.23
Hydrolysis	-1	$3.5505 \times 10^5$	71.90

From data above, the kinetic parameters using the modified LHHW model can represent the reaction rate for different water concentrations (1.9 – 17.9 %wt) and temperature between 35-65°C. Therefore, this model can be applied to our

investigation of the effect of water for Amberlyst-15 catalyzed esterification in the hybridized reactive distillation.

### 3.2.2 Base catalyst (Calcium oxide, CaO) for transesterification

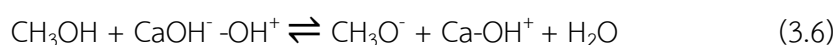
Biodiesel is normally produced by a transesterification process of vegetable oils with methanol. The overall transesterification reaction already given in chapter 2. (Eq 2.4) and the side reaction (Eq 2.6) could be occurred with the presence of water content in feedstock. Moreover, the presence of water and FFA in oil can be emulsified to obstacle the transesterification [34].



From above reaction, many researches [7, 35-37] neglected the effect of presence of water on transesterification rate. The approach kinetic rate is derived based on the elementary rate law in Eq 3.4.

$$-r = \frac{-d[\text{TG}]}{dt} = k[\text{TG}][\text{ROH}]^3 \quad (3.4)$$

Although, many researches avoid of water effect but some research has been reported. Liu et al. [14] found that the effect of trace amount of water existing in the reaction mixture (< 2.8 %wt oil) can accelerate the rate of transesterification because basic site of CaO solid base catalyst extracts  $\text{H}^+$  from  $\text{H}_2\text{O}$  to form surface  $\text{OH}^-$  Eq 3.5. Then, the  $\text{OH}^-$  extracts  $\text{H}^+$  from methanol to generate methoxide anion and  $\text{H}_2\text{O}$  Eq 3.6. That methoxide anion is strongly basic than CaO and has high catalytic activity in transesterification.



The results show that the biodiesel yield increased with the rising water content in methanol. However, the water content in reaction mixture should be kept

less than 2.8 %wt to prevent soap formation (Figure 3.7). Figure 3.8 also presented the significant decrease in biodiesel yield, when water content was more than 2 %wt.

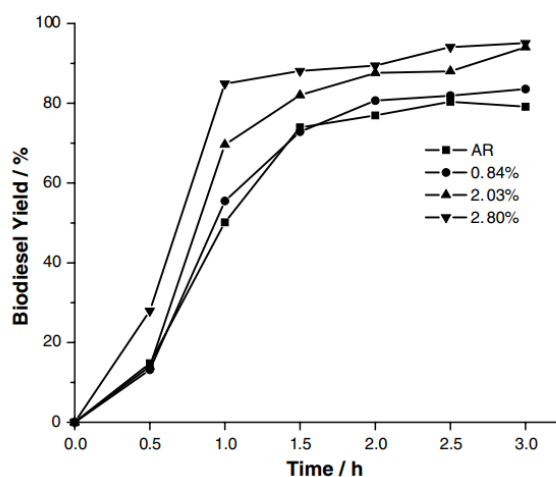


**Figure 3.7** Effect of water content of methanol on biodiesel yield. CaO/Oil mass ratio: 8%wt reaction temperature 65°C; methanol/oil molar ratio 6:1[14]

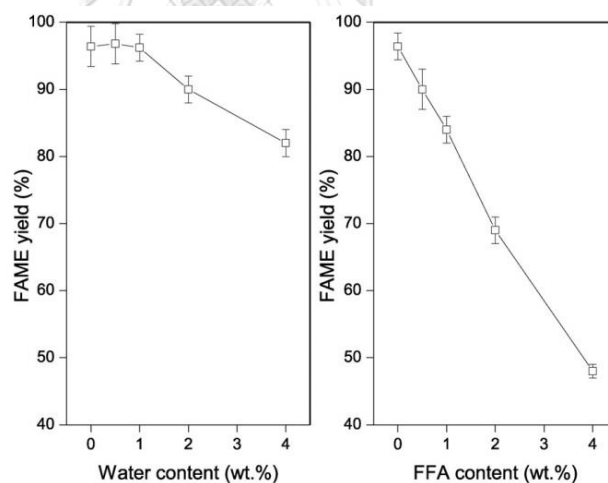


**Figure 3.8** The effect of water (a, left) and FFA content (b, right). Conditions: reaction time, 2.5 h; methanol to oil molar ratio of 9; catalyst loading, 7%wt; temperature 65°C [38]

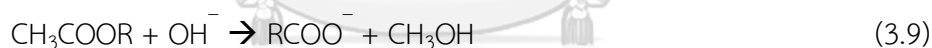
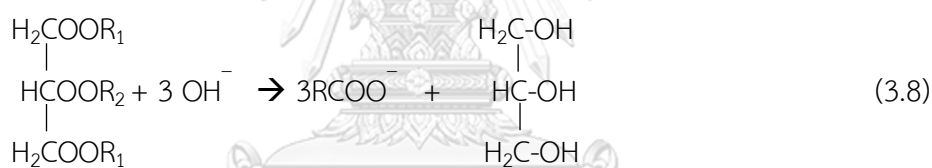
However, this previous research proposed only the mechanism of the presence of a trace amount of water during transesterification over CaO which did not take account the concentration of water into the kinetic model. Therefore, in this

work is going to propose kinetic rate model accounting the water effect for CaO catalyzed transesterification.

### 3.2.3 Base catalyzed saponification

In alkali-catalyzed homogeneous transesterification, hydroxides and methoxides of sodium and potassium is commonly used. There also can saponification of the oil (TG) or the fatty acid methyl esters (FAME) (Eqs 3.8 and 3.9) to form soap. This occurs alongside the main reactions due to the existence of the hydroxide-alkoxide equilibrium (Eq 3.7). This equilibrium can shifts towards the formation of hydroxide when the water content was increased.

The formation of soap leads to emulsification, which renders the downstream separation of glycerol very difficult.



Saponification of alkyl esters can occur in aqueous hydroxide solutions [39], mixtures of water and soluble organic solvents. It has been reported that saponification of carboxylic acid esters in hydroxide solutions is a bimolecular reaction, which is first order for ester and hydroxide ions [39, 40]. Hydroxide ions attack the carbonyl to form a tetrahedral intermediate, which then decomposes to the products (Figure 3.9a).

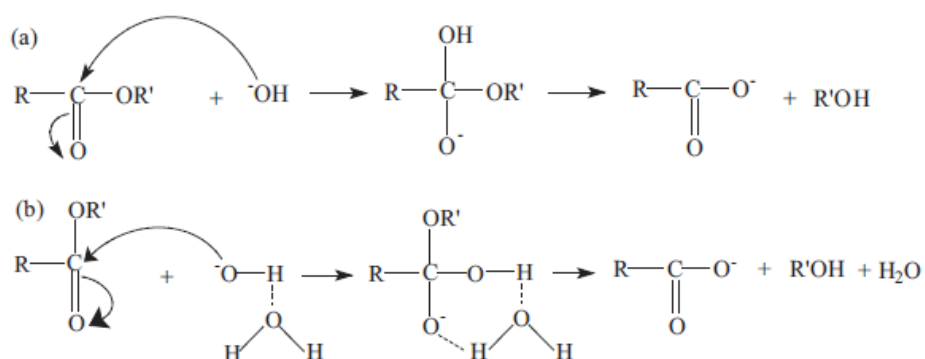
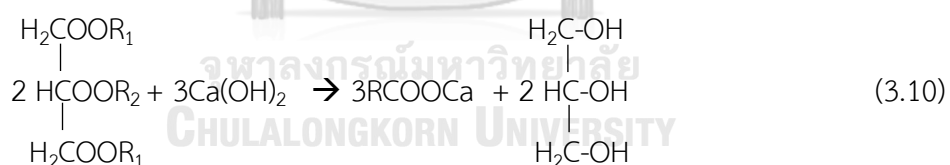


**Figure 3.9** Saponification of alkyl esters (a) reaction mechanism for alkyl esters saponification; (b) bimolecular collision by solvated hydroxide ions to form H-bond stabilized tetrahedral intermediate [41]

However, the recent studies [42, 43] found that the reactions did not occur via simple bimolecular collisions, but rather required a molecule of water to form the tetrahedral intermediate. This indicates that a water molecule stabilizes the transition-state complex through hydrogen bonding (Figure 3.9b). Such hydrogen bonding could also be provided by other protic solvents such as simple alcohols.

For saponification reaction in the presence of CaO is caused by  $\text{Ca}(\text{OH})_2$  which has base properties [44, 45]. The followings are the reaction of the saponification as shown in Eqs 3.10 and 3.11.



## Chapter 4

### Kinetic experiment and simulation

#### 4.1 Kinetics of esterification

##### 4.1.1 Materials

Reactants are oleic acid from Vicchi Enterprise and methanol analytical grade from QRëC (99.8% purity). Amberlyst-15 was purchased from Sigma-Aldrich used for esterification and was dried at 100°C for overnight before used. Analytical agents is methyl valerate as analytical grade from Sigma-Aldrich (99% purity) and propanol was used as internal standard and solvent respectively for GC analysis.

##### 4.1.2 Experimental

The experiments were performed in a 3-neck-flask with condenser and thermometer into an oil bath to control temperature of reaction mixture at 60 °C using stirring speed of 600 rpm. Prior to the experiment, oleic acid and methanol were pre-heated to the desired temperature of 60°C in separated vessel. Then, the catalyst was added to the reaction mixture at desired temperature. The reaction time was started. Sample of 1 mL was taken every 30 min and centrifuged to separate the catalyst from reactant and product to stop reaction.

#### 4.2 Kinetics of transesterification

From the literature review in chapter 3, the presence of water during CaO catalyzed transesterification has effect of counter balancing effect. For instance, a trace amount of water could generate new active sites to accelerate transesterification while large amount of water could decrease transesterification rate with soap formation. Therefore, the kinetic model accounting of the water effect on the rate to biodiesel production was proposed by using triolein as triglyceride model compound and methanol. This proposed kinetic model will be further used to investigate the simulation of water effect on the operating parameter in a hybridized RD to produce biodiesel from WCO.

#### 4.2.1 Determination of the empirical rate model

The various concentration in unit mol/L of triolein [TG] and methanol [MeOH] with amount of water (H<sub>2</sub>O) based on oil weight is shown in Table 4.1. The experimental condition was 1 atm, 60°C and speed stirring 700 rpm to avoid mass transfer limitation.

Determining rate law depend on H<sub>2</sub>O for constant concentration of TG and MeOH (run 1-7)

$$r_{\text{FAME}} = \frac{C[\text{H}_2\text{O}]^x}{1+d[\text{H}_2\text{O}]^y}, \quad C = [\text{TG}]^w \cdot [\text{MeOH}]^z$$

Determining rate law depend on TG for constant concentration of MeOH and H<sub>2</sub>O (run 4, 8-12)

$$r_{\text{FAME}} = A[\text{TG}]^w, \quad A = \frac{[\text{MeOH}]^z \cdot [\text{H}_2\text{O}]^x}{1+d[\text{H}_2\text{O}]^y}$$

Determining rate law depend on MeOH for constant concentration of TG and H<sub>2</sub>O (run 4, 13-15)

$$r_{\text{FAME}} = B[\text{MeOH}]^z, \quad B = \frac{[\text{TG}]^w \cdot [\text{H}_2\text{O}]^x}{1+d[\text{H}_2\text{O}]^y}$$

**Table 4.1** Initial mole ratio and percent water of each run

Run	TG (mol)	MeOH (mol)	H <sub>2</sub> O %wt oil
1	1	6	0
2	1	6	1
3	1	6	2
4	1	6	5
5	1	6	8
6	1	6	10
7	1	6	15
8	1.35	6	5
9	1.25	6	5



Run	TG (mol)	MeOH (mol)	H <sub>2</sub> O %wt oil
10	0.9	6	5
11	0.75	6	5
12	0.65	6	5
13	1	1	5
14	1	3	5
15	1	9	5

#### 4.2.2 Determination of activation energy (E<sub>a</sub>)

Determine E<sub>a</sub> of CaO catalyzed transesterification of triolein in the temperature range of 50 to 70 °C and condition are [TG] = 1 mol/L , [MeOH] = 6 mol/L and [H<sub>2</sub>O] 5%wt oil

#### 4.2.3 Materials

Triolein was used as a reactant from SHANGHAI TERPPON CHEMICAL (99.5% purity) while methanol with analytical grade from QRc (99.8% purity). Calcium oxide (CaO) catalysts was obtained from Sigma-Aldrich (96% purity) calcium oxide fine powder catalyst was calcined in a furnace with the heating rate 15°C/min to 900°C and hold for 5 h then kept in desiccator cabinet before use. Analytical agents were used as well as esterification reaction.

#### 4.2.4 Experimental

The experiments were performed in the same equipment of esterification reaction but using stirring speed of 800 rpm. Prior to the experiment, triolein and methanol were pre-heated to the desired temperature of 50-70°C in separated vessel. Then, the catalyst was added to the reaction mixture at desired temperature. The reaction time was started. Sample of 1 mL was taken every 15 min and centrifuged to separate the catalyst from reactant and product to stop reaction.

### 4.3 Sample analysis

The sample solution was then analyzed by gas chromatography from Shimadzu GC-2010 Plus with DB-WAX capillary column and detected by flame ionization detector (FID). Methyl valerate was used as internal standard. The column temperature program starts at 40 °C with holding time 3 min with ramp rate 15 °C/min to 235 °C holding time 2 min, the ramp rate 10 °C/min to 260 °C with holding time 20 min.

### 4.4 Simulation

Aspen Plus® version 8.0 was used to simulate the effect of water on the operating parameter. Based on the previous work [13], it was reported that the Dortmund modified UNIFAC model was the most suitable model for prediction of the physical equilibria properties of various mixtures associated with the design of biodiesel processes. The RADFRAC model was extensively used in the design of RD columns. RADFRAC relies on an equilibrium stage model and is capable to deal with ideal and non-ideal vapor-liquid equilibrium (VLE) and vapor-liquid (I)-liquid (II) equilibrium (VLLE).

Verification of kinetic model for Amberlyst-15 catalyzed esterification using a Langmuir-Hinshelwood-Hougen-Watson (LHHW) approach derived from Steinigeweg and Gmehling [8] was carried out by comparing the simulation results with the experimental results performed in this study. The verified kinetic model was then further applied in the simulations of hybridized RD in the esterification section (top section) and the empirical kinetic model of CaO catalyzed transesterification with accounting the effect of water would be used for transesterification (bottom section).

The effect of water on the operating parameter of reactive distillation in terms of water contain in feedstock, number of stage and feed location to obtain the biodiesel yield and purity according to EN 14214 (FAME  $\geq$  96.5%) was used to simulate and compare with the base case from the previous work [13].

## Chapter 5

### Results and discussion

#### 5.1 Esterification

##### 5.1.1 Kinetic model verification for esterification of oleic acid

Figure 5.1 shows the verification results of kinetic model of Amberlyst-15 catalyzed esterification. Dots and continuous line represent the experimental results and the results from simulation using the proposed kinetic rate model in chapter 3 (Eq 3.3).

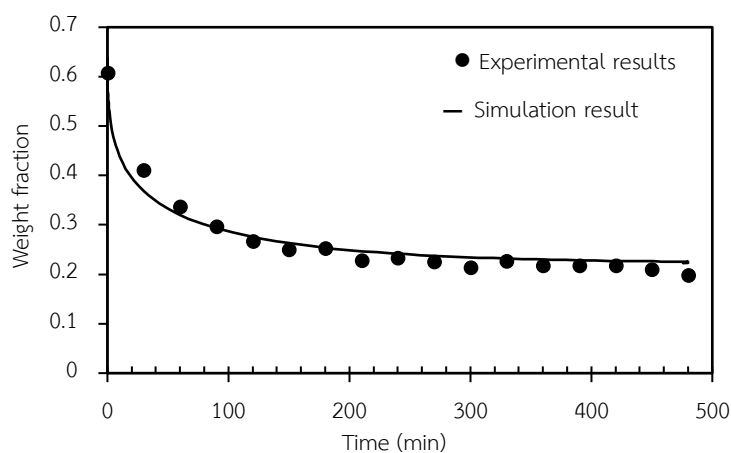


**Figure 5.1** Kinetic model fitted eq.3.3 (continuous line) and experiment (•) condition are  $T=60\text{ }^{\circ}\text{C}$  methanol to oil ratio 5:1,  $X_0\text{ water}=0.019$

The results indicated that there was less significant difference with the maximum error about 13% in the experimental results (esterification of oleic acid and methanol) and the simulation result using the kinetic model provided by Steinigeweg and Gmehling [8] (Appendix C). Although, oleic acid composes of C18:1 having more carbon atom than that of decanoic acid (C10:0), these fatty acids showed the similar reactivity using Amberlyst-15 catalyzed esterification investigated by Banchemo and Gozzelinolt [46]. They reported that the quite similar conversion profiles versus time for the 1:1 esterification of the different acids (C12-C18) with methanol using Amberlyst-15 catalyzed esterification at  $70^{\circ}\text{C}$ .

Therefore, this kinetic model [8] was further used in simulations of biodiesel production in the hybridized RD.

### 5.1.2 Validation of esterification in RD

Based on the kinetic constants and activation energies for the esterification of decanoic acid using Amberlyst-15 reported by Steinigeweg and Gmehling [8] as shown in Table 3.1, this work used oleic acid as feedstock in the RD. Therefore, the validation of acid conversion as a function of reflux ratio was also performed as shown in Figure 5.2. It was found that the obtained simulation results of the various reflux ratios using kinetic model of oleic acid was close to experimental results of decanoic acid obtained from Steinigeweg and Gmehling [8] with the maximum error about 15%.

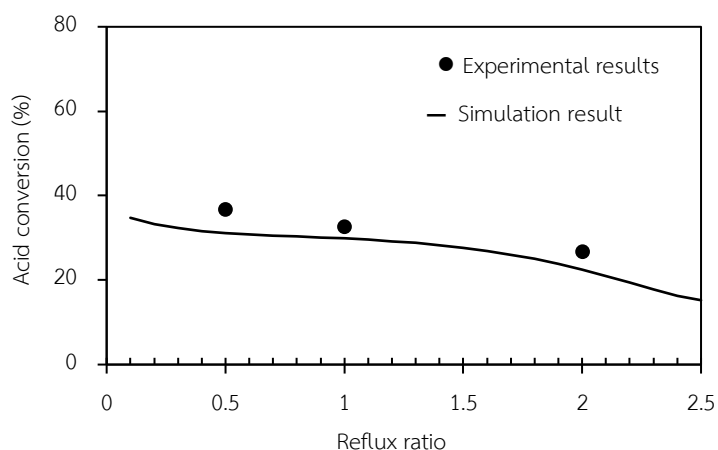


**Figure 5.2** Acid conversion as a function of reflux ratio. Experimental data (•) [8] and simulation results (continuous line)

Banchero and Gozzelino [47] proposed the esterification of stearic acid with methanol ( $P = 4$  atm, number of reactive stages from 3 to 22, temperature of the acid feed of  $160^{\circ}\text{C}$ , temperature of the methanol feed of  $104.5^{\circ}\text{C}$ ). This result showed that the higher conversions and lower energy consumption can be achieved by operating at low reflux ratio values. For the RD configuration, the reflux functions like an internal recycle of a methanol–water mixture whose composition depends on

the reflux ratio. Higher reflux ratio values result in higher amounts of liquid flowing through the column which involves higher heat duties both at the reboiler and condenser. [47]

## 5.2 Transesterification

### 5.2.1 Determining the rate reaction of Transesterification in the presence of water

Kinetics of transesterification was calculated based on the concentration of produced FAME at the initial rate (0-60 min) to determine the forward transesterification rate in the presence of water including the reaction order of TG and methanol on the rate expression.

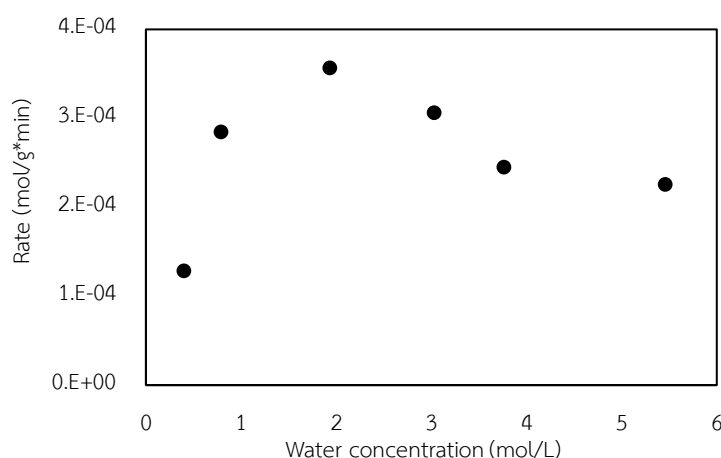


**Figure 5.3** The effect of concentration of water on the initial transesterification rate

The effect of the presence of water on the initial rate is shown in Figure 5.3. The highest initial rate of reaction was obtained when using the 5%wt of water based on triolein (TG) weight. The water concentration of 0-2 mol/L as corresponding to 0-5 %wt was introduced in the reaction mixture, the increase in the initial rate was obtained. This is corresponding to the previous work with using CaO catalyzed transesterification. Water can promote the rate of transesterification by generation of

the methoxide anion form the extracts  $H^+$  from water to form surface  $OH^-$  on CaO surface [14].

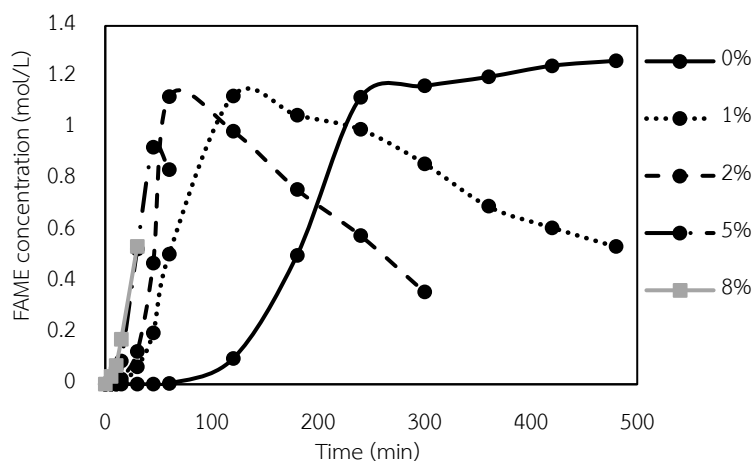


**Figure 5.4** Results from experimental run 1-5, the concentration of FAME profile along the reaction time.

Figure 5.4 shows the FAME concentration profiles for CaO catalyzed transesterification of triolein using various water content in the range of 0 to 8 %wt. The induction period of FAME concentration profiles was found to be reduced from 60 to 15 min with increase amount of water content from 0 to 8 %wt. However, the present of water only 1%wt, the FAME concentration was reduced after reach the maximum value due to the saponification as a side reaction took place and the emulsion phase of water and oil also performed [14].

The empirical kinetic model in the presence of water was also performed in Eq 5.1 (Appendix D).

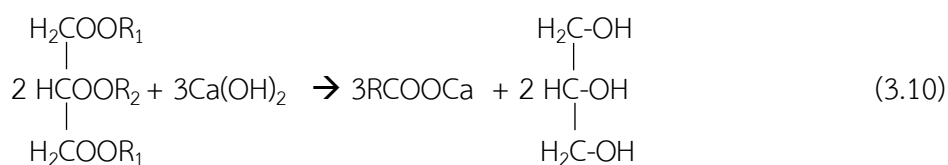
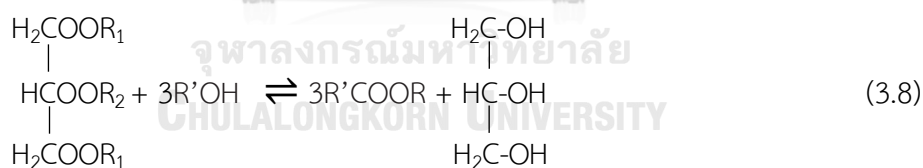
$$r_{\text{FAME}} = \frac{7.78 \times 10^{-5} [\text{H}_2\text{O}]^{0.5}}{1 + 0.46 [\text{H}_2\text{O}]} [\text{TG}]^{0.5} [\text{MeOH}] \quad (5.1)$$

It was found that the presence of water gave both the counter balance effect on the initial transesterification rate. The presence of a trace amount of water less than 1%wt (0.789 mol/L) could give rise of the forward transesterification rate because the denominator term of 1 was greater than  $0.46[\text{H}_2\text{O}]$  resulting in the

increase in the forward rate of reaction. While the increase amount of water content more than 1 %wt, the denominator term of 1 was less than  $0.46[\text{H}_2\text{O}]$  resulting in the decrease in the forward rate.

This should be noted that the FAME concentration was significantly decreased after reaching the maximum value. This is because of the saponification of TG and FAME with the hydroxyl group on the CaO surface and the presence of emulsion phase of water and TG [14]. Therefore, the presence of side reactions as a saponification with the water concentration of 1-8 %wt, can be found. This system should be three overall reactions involving in the corresponding FAME concentration profile.

The possible three overall reactions including of overall forward transesterification, overall reverse transesterification and saponification were proposed. It was found that transesterification in this work was used for overall reaction rate (Eq 3.8). Eqs 3.10 and 3.11 were represent the mechanistic partway of CaO with the presence of water to generate  $\text{Ca}(\text{OH})_2$  and react with TG or FAME to produce soap.



To simulate the concentration profile of FAME, this requires at least 3 equations of rate reactions including of forward transesterification ( $r_1$ ), backward transesterification ( $r_2$ ) and saponification ( $r_3$ ) using a built-in ODE45 solver in MatLab

(Appendix D). Eqs 5.8 to 5.13 were used to derive the rate model and results were shown in Figure 5.5.

$$r_1 = k_1 [\text{TG}]^{0.5} [\text{Me}] \quad (5.8)$$

$$k_1 = \frac{kT[\text{H}_2\text{O}]^{0.5}}{1+30[\text{H}_2\text{O}]} \quad (5.9)$$

$$k(T) = k_0 \exp\left(\frac{-E_a}{RT}\right) \quad (5.10)$$

$$r_2 = \frac{k_1}{K_{\text{eq}}} [\text{FAME}][\text{GLY}] \quad (5.11)$$

$$r_3 = k_2 [\text{FAME}]^{1.5} \quad (5.12)$$

$$k_2 = 0.003[2\text{OH}^-] \quad (5.13)$$

$k_1$  was the reaction rate constant for the forward transesterification with taking account of the effect of water.  $K_{\text{eq}}$  was the equilibrium reaction rate constant for transesterification.  $k_2$  including of the dissociation of water or methanol to hydroxyl group was the reaction rate for saponification of FAME.

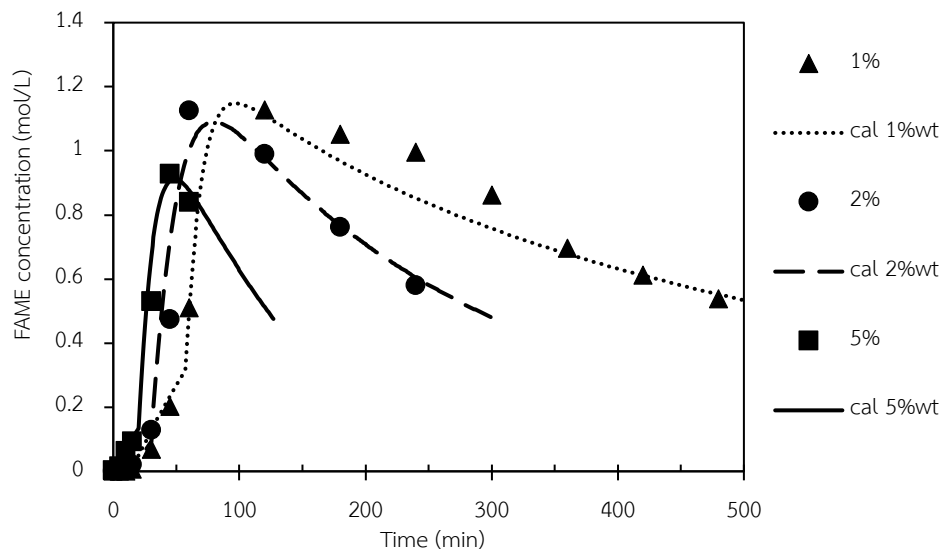


**Figure 5.5** Result of the concentration of FAME profile along the reaction time of experiment (▲1%wt, ■2%wt and ●5%wt of water content) and calculation from MatLab (... 1%wt, - - 2%wt and — 5%wt of water content)



Figure 5.5 shows the simulation results of the proposed kinetic model including of 3 reactions ( $r_1$ -forward transesterification,  $r_2$ -backward transesterification and  $r_3$ -sponification) was fitted with the experimental results for the water content of 1 to 5 %wt which refers to the water concentration of 0.397 to 1.932 mol/dm<sup>3</sup> in the reaction mixture.



$$\text{Keq} = \frac{[\text{FAME}]^3 [\text{GLY}]}{[\text{TG}] [\text{MeOH}]^3} \quad (5.14)$$

Generally, at equilibrium condition, the rate of forward reaction should be equal to the rate of backward reaction. However, this work found that FAME can react with CaO in the presence of water to generate saponification as a side reaction as can be seen the remarkably drop in the FAME concentration when it reached the plateau.

The reaction rate parameters for transesterification of triolein with the presence of 5 %wt water content in the reaction temperature of 50 to 70°C including of  $k_0$  and  $E_a$  determining from Arrhenius plot were equal to 47.2 and 16 kJ/mol, respectively. The Arrhenius plot is shown in Figure 5.5.

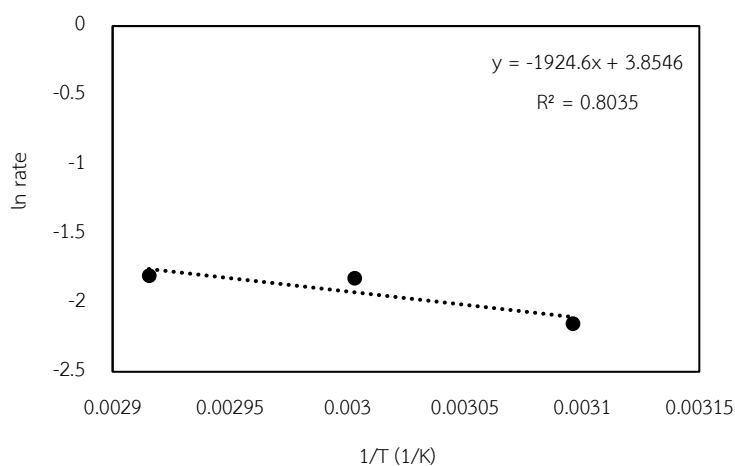


**Figure 5.6** Result between ln rate and 1/T in Kelvin

**Table 5.1** Kinetic constants from CaO catalyzed transesterification

Oil feed	Reaction condition				Kinetic model / Reaction order	Rate constant	Ea (kj/ mol)	Ref
	T (°C)	Molar ratio	Cat (%wt)	Time (hr)				
Palm oil	65	9:1	5	1	$-r_a = k C_a$	$k=0.0119$ (/min)	-	[36]
Soybean oil	125- 200	9:1	3	2.5	Pseudo-first order	$k_0=29.9$ (/min)	30.7	[26]
Soybean oil and waste cooking oil	65	10:1	1	2	First with respect to TG	$k=0.044$ (/min)	-	[48]
Sunflower oil	60	6:1	1-10	2	Pseudo-first	$k=0.07$ (/min)	-	[49]
Triolein with 5%wt water	50- 70	6:1	10	1	$r_1 = \frac{k(T)}{30[H_2O]^{0.5}}$ * $[TG]^{0.5}[Me]$	$k_0=47.2$ (/min)	16.0	This work
Triolein No water	50- 70	6:1	10	1	pseudo-second order	$k_0=15.0$ (/M*min)	36.1	This work

The comparison of  $k$  or  $k_0$  and  $E_a$  with other researches was found that the rate constant for transesterification of triolein with water was highest because the positive effect of the presence of water in the reaction mixture can accelerate the initial rate of transesterification as can be seen from Figure 5.4. The presence of water in feedstock can reduce induction period due to the dissociation of water can activate the CaO catalyst with the generation of methoxide ion as the active site for transesterification [ref].

However, this should be noted that the presence of water also causes the serious situation of the transesterification for biodiesel production even using heterogeneous catalyst (CaO) for long reaction period. Therefore, the operation condition of hybridized RD must be avoided the water contamination more than 1

%wt for CaO catalyzed transesterification. Therefore, the kinetic model of CaO catalyzed transesterification of triolein in the absence of water also investigated in the next section.

### 5.2.2 Determining the rate reaction of Transesterification in the absence of water

In order to determine the kinetic of transesterification of triolein in absence of water. Assuming, the concentration of methanol is constant because of using methanol to oil ratio of 6 to 1 which larger than the theoretical of transesterification. The integration method was used to determine the reaction rate constant (k) as derived from Eqs 5.16 to 5.18. It was found that the pseudo second-order of TG was fitted to the experimental result (Figure 5.7) with the reaction rate constant (k) of  $3.30 \times 10^{-5}$  L/mol min for the reaction temperature of 50-70°C.

$$r_{TG} = -k [TG]^2 \quad (5.16)$$

$$\frac{dC_{TG}}{C_{TG}^2} = -kt \quad (5.17)$$

$$\frac{1}{C_{TG}} = kt + \frac{1}{C_{TG,0}} \quad (5.18)$$

Then, k was the reaction rate constant, t was time in min,  $C_{TG}$  was triolein concentration at that time in mol/L and  $C_{TG,0}$  initial concentration of triolein.

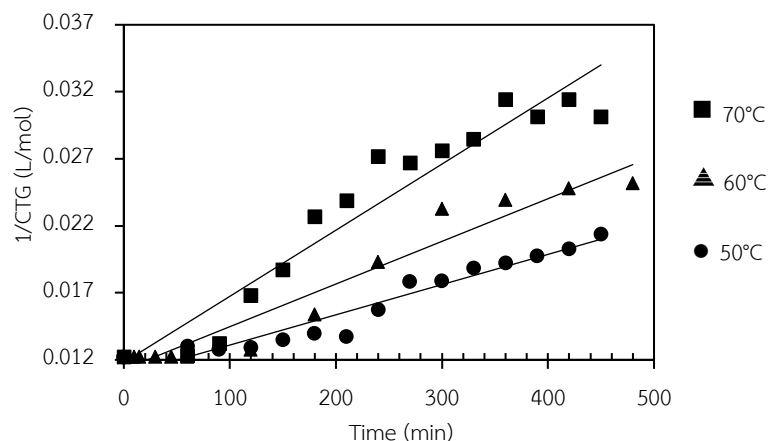


**Figure 5.7** Pseudo second-order reaction model of transesterification at various temperature 50-70°C.

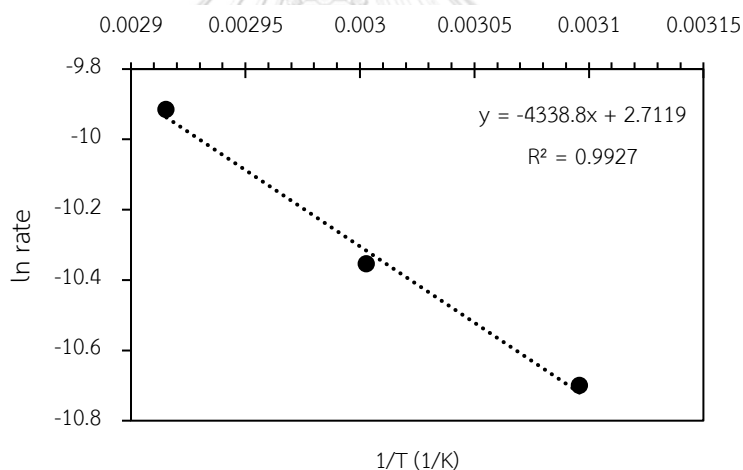


**Figure 5.8** Result between  $\ln$  rate and  $1/T$  in Kelvin

The reaction rate parameters in the reaction temperature of 50 to 70°C including of  $k_0$  and  $E_a$  determining from Arrhenius plot were equal 15 and 36 kJ/mol, respectively. The results show in Figure 5.8 and Table 5.1. The rate constant was in agreement to that reported by Pasupulety et al. [26] but slightly lower because the lower reaction temperature range was used in this work.

### 5.3 Reactive distillation: effect of design parameter

The schematic diagram of ester-transesterification in a single reactive distillation column is shown in Figure 5.9.

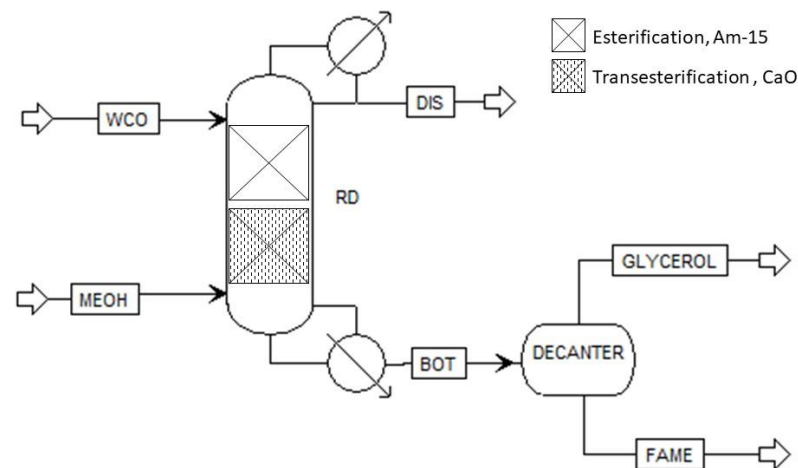


**Figure 5.9** Ester-transesterification in reactive distillation column.

Petchsoongsakul et al. [13] reported that the operation of hybridized RD at 1 bar required 4 stage for esterification and 20 stage for transesterification of oil contaminated FFA. Therefore, this condition was also preliminary used for this study.

This section was aimed to determine the optimal condition for biodiesel production in the hybridized RD. The effect of water on the operating parameter of hybridized RD in terms of water containing in feedstock, number of stage and feed location to obtain the biodiesel yield and purity according to EN 14214 (FAME content  $\geq 96.5\%$ ) was considered to simulate and compared to the other scenario case. The kinetic model of esterification was used LHHW from Eq 3.3 for both cases. The effect of water content on the transesterification rate using Eqs 5.8-5.10 was presented in case 1 and compared to the transesterification rate in the absence of water (case 2) as shown in Table 5.2. It was found that the activation energy obtained from the transesterification in the presence of water was lower than that of

the absence of water because the presence of less amount of water can generate the methoxide ion as homogeneous catalyst to catalyze transesterification [14].

**Table 5.2** Kinetic model used for simulation of hybridized RD

Reaction	Case 1		Case 2		Ref
	$k_0$ (mol/ g min )	$E_a$ (kJ/mol)	$k_0$ (mol/ g min)	$E_a$ (kJ/mol)	
Kinetic esterification	$1.91 \times 10^8$	72.23	$1.91 \times 10^8$	72.23	[8]
Kinetic hydrolysis	$2.13 \times 10^7$	71.90	$2.13 \times 10^7$	71.90	[8]
Kinetic forward transesterification	47.2	16	15	36	This work
Kinetic backward transesterification	$3.10 \times 10^{-2}$	16	$9.88 \times 10^{-3}$	36	This work
Kinetic saponification	47.2	16	-	-	Thus work (Appendix E)

Table 5.3 shows the all components in feed of waste cooking oil (WCO) model compound in mass fraction and mole flow and methanol (MEOH) in mole flow using for the simulation. In the absence of water in WCO as a based case, the methanol to oil molar ratio was used 6 to 1. However, this molar ratio was not appropriate for WCO feedstock with water contamination. Therefore, the difference in mole flow of methanol was used with various amount of water content by fixed the constant methanol to TG molar ratio of about 7. As can be seen from Table 5.3, the water content in WCO was increased from 1 to 8%wt, the mole flow of TG was significantly decreased.

**Table 5.3** WCO feedstocks and methanol composition

WCO with various Water content (%wt)	Component Mass fraction			Component Mole flow (kmol/h)			Feed Methanol (kmol/h)
	TG	FFA	Water	TG	FFA	Water	
	0	1	0.1	0	0.76	0.24	
1	1	0.1	0.01	0.55	0.17	0.27	4
2	1	0.1	0.02	0.44	0.14	0.43	3
5	1	0.1	0.05	0.27	0.08	0.65	2
8	1	0.1	0.08	0.19	0.06	0.75	1.5

### 5.3.1 Hybridized RD in the presence of water for transesterification section

This hybridized RD can produce biodiesel yield of 99.6% using a stage residence time of 5 min because the low activation energy (16 kJ/mol) obtained from CaO catalyzed transesterification in the presence of water using reflux ratio of 0.1 and reboiler duty 26.9 kW. Liquid mass fraction of all components are shown in Figure 5.10. TG mass fraction was immediately reduced at stage 6 as the first stage of transesterification section. Unfortunately, the biodiesel purity was lower than 96.5% as presented in Figure 5.11. This is because the saponification as a side reaction took place resulting in generation of the emulsion phase of water and oil in bottom of reactive distillation. Therefore, the separation of glycerol and biodiesel could not be performed in the decanter resulting in the lower biodiesel purity. The effect of stage residence time of hybridized RD on the biodiesel yield and purity was also investigated as illustrated in Figure 5.12. When the stage residence time was varied from 5 to 60 min, the biodiesel yield was higher than 96.5% while biodiesel purity was lower as about 80% which could not meet the EN14214 standard. This simulation results confirmed that the serious separation of biodiesel and glycerol with the presence of saponification. This can be concluded that the presence of

water in transesterification should be limited to only 1%wt to avoid the saponification as serious side reaction.

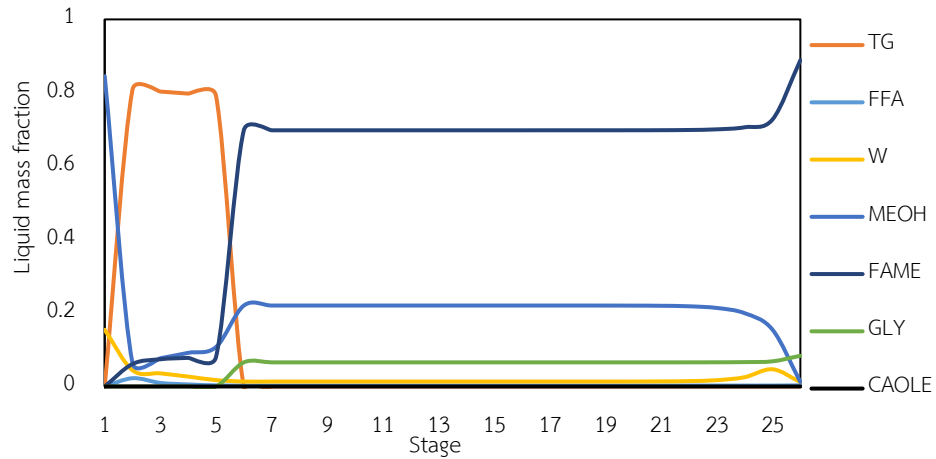


**Figure 5.10** Liquid mass fraction in hybridized RD using TG with water content 5 %wt, methanol to TG molar ratio of 7:1, reflux ratio of 0.1 and residence time 5 min.

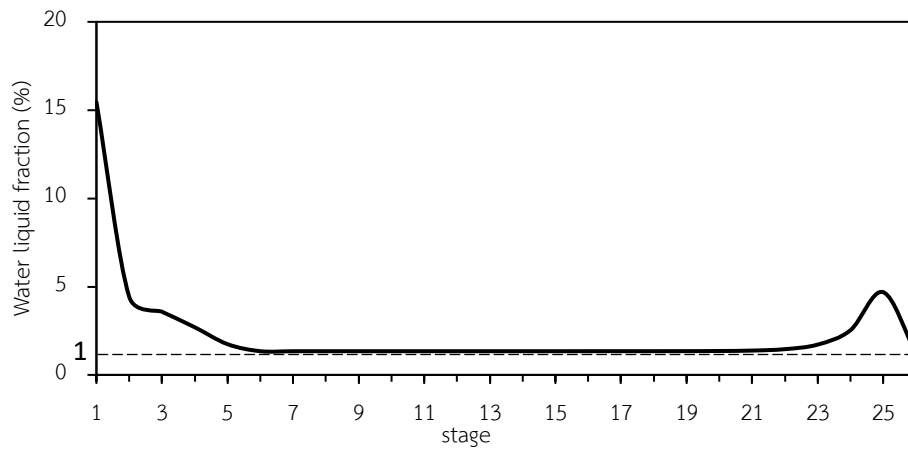


**Figure 5.11** Percent of water in liquid fraction in a hybridized RD using TG with water content 5 %wt, methanol to TG molar ratio of 7:1, reflux ratio of 0.1 and stage residence time of 5 min.



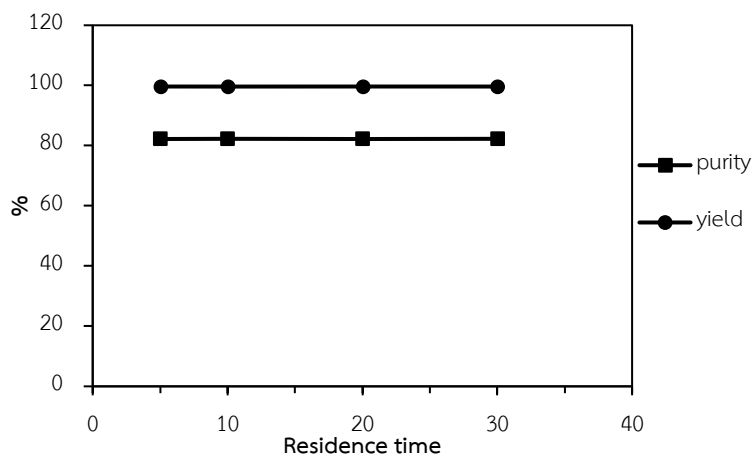


**Figure 5.12** Biodiesel yield and purity as function of residence time using methanol to TG molar ratio of 7:1 and reflux ratio of 0.1

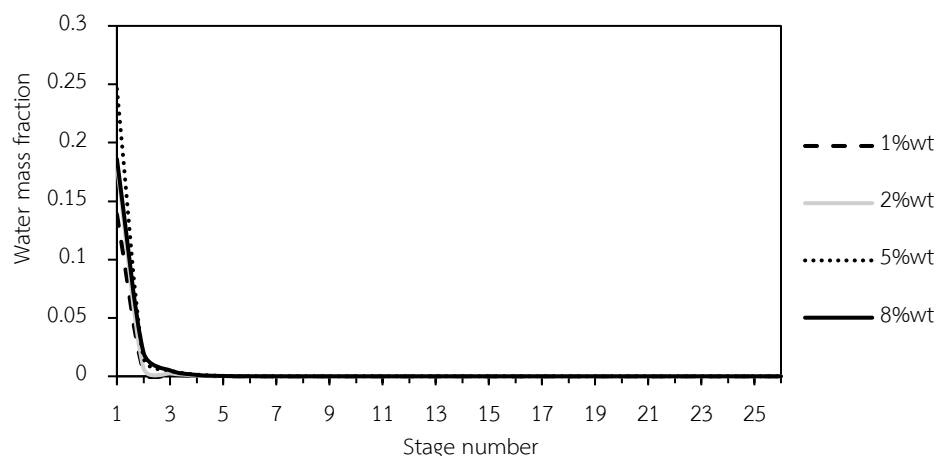
### 5.3.2 Hybridized RD in absence of water in transesterification section

The previous section showed the serious problem of biodiesel separation resulting in low biodiesel purity with the presence of water in transesterification section. Therefore, the water contamination in transesterification section for biodiesel production in hybridized RD must be limited (less than 1 %wt of water content). The pseudo second order of CaO catalyzed transesterification was used to simulate the effect of water on the operating parameter of hybridized RD in terms of water containing in feedstock, number of stage and feed location to obtain the biodiesel yield and purity according to EN 14214 (FAME  $\geq$  96.5%) for this case.

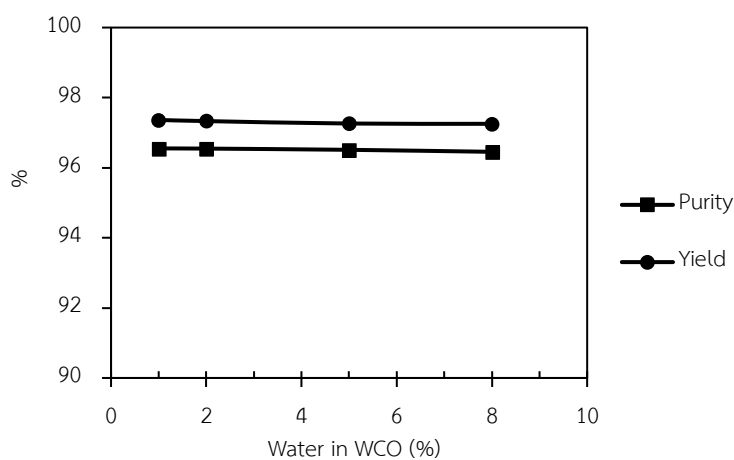
#### 5.3.2.1 Water content in feed WCO

The simulation results of using WCO feedstocks with the water content of 1-8%wt were illustrated in Figure 5.13. The water was vaporized to the top of column even the presence of 8%wt water content in WCO. This might be due to the big different boiling point between water and triolein in WCO [12]. Therefore, in transesterification section, the trace of amount of water could be negligible. The produced FAME purity constrain was selected to conform to EN standard of biodiesel with 96.5%. Based on this result, the hybridized RD could be a suitable reactor for

biodiesel production. However, this should be noted that the amount of water must be removed before introducing to the transesterification section.



**Figure 5.13** Water mass fraction in reaction section different water content in feedstock 1-8 %wt.



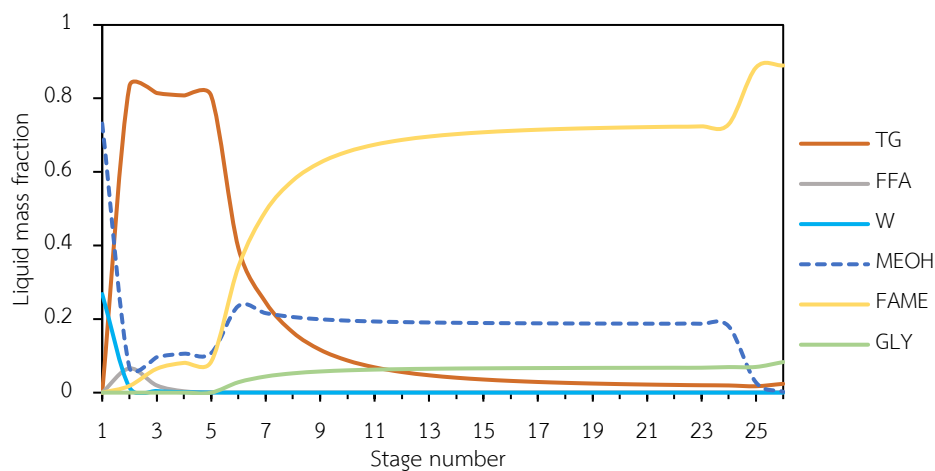
**Figure 5.14** Biodiesel yield and purity as function of water content in WCO using methanol to TG molar ratio 7:1 and reflux ratio 0.1

Figure 5.14 presents the effect of water content in WCO feedstocks on the biodiesel yield and their purity using methanol to TG molar ratio of 7 to 1, reflux ratio of 0.1 and stage residence time of 60 min. As can be seen, this case using longer residence time could produce biodiesel yield more than 96.5% as compared to the

case using kinetic model with presence of water because of the lower transesterification as found the kinetic model. However, this case can use a decanter to separate biodiesel from glycerol as a simple separation unit. It was found that there were no significant differences in biodiesel yield and purity with increase of amount of water because the high FAME yield via transesterification was also obtained for WCO feedstocks with water content from 1 to 8 %wt and the water was also vaporized to the top of hybridized RD. This finding is in agreement to our previous work using triglyceride with various amount of FFA and the presence of water derived from esterification of FFA. This work found that water and methanol were vaporized to the top of column and not flown down to the transesterification section as in the bottom of column [13]

#### **5.3.2.2 Number of stages**

Based on the previous results, the hybridized RD with various amount of water content from 1 to 8 %wt were used 26 total stages including 4 stages for esterification, 20 stages for transesterification, rectifying and stripping stages. Figure 5.10 shows the liquid mass fraction profile of all components in hybridized RD for 5%wt of water content in WCO feedstock. At the top section, FFF was consumed via esterification resulting to reduce in mass fraction of FFA from stage 1 to 5. TG, on the other hand, this component was converted to FAME via transesterification section with CaO catalyst packing from stage 6 to 25. The excess methanol was completely separated at the last stage as the re-boiler stage and vaporized to the first stage at the top of column resulting to obtain high FAME purity in this hybridized RD.



**Figure 5.15** Liquid mass fraction in a reactive distillation using TG with water content 5 %wt, methanol to TG molar ratio of 7:1 and reflux ratio of 0.1

The effect on number of stage on the biodiesel yield and purity was also investigated to minimize the number of stage with producing biodiesel purity according to EN14214 standard. The simulation results showed that the esterification section using Amberlyst-15 as a catalyst required only 4 stages to reduce amount of FFA from 10%wt to less than 1%wt as can be seen in Figure 5.15. Therefore, the number of stages for transesterification should be further investigated as shown in Figure 5.16. It was found than the minimum number of transesterification stage using CaO as a catalyst was 20 stages to meet the biodiesel purity of 96.5% corresponding to the EN14214 standard. The biodiesel yield and their purity were significantly reduced with decrease in the number of transesterification stage less than 20 stages. This is because the CaO catalyzed transesterification has lower catalytic activity compared to NaOH as a homogeneous catalyst [13]. This process required more reaction as well as number of reaction stage to complete reaction resulting to lower biodiesel yield and purity with reducing of number of transesterification stage. However, the homogeneous catalyst could be appropriate for the hybridized RD in terms of economic point of view and the green and sustainable process.

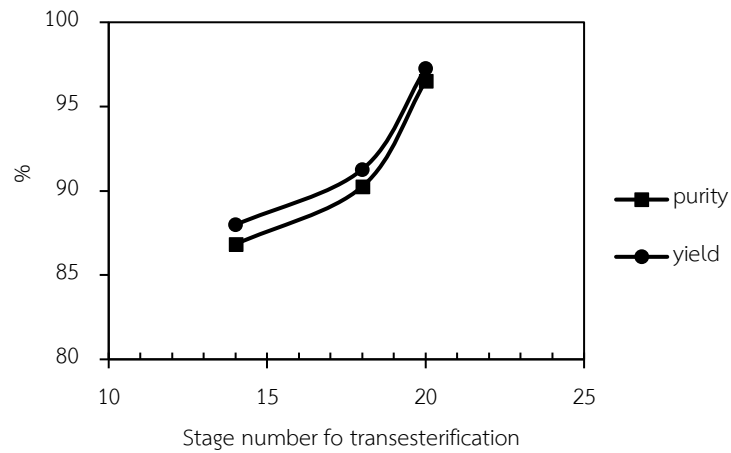


**Figure 5.16** Biodiesel yield and purity as function of number stage for transesterification using methanol to TG ratio 7:1, water content of 5%wt and reflux ratio 0.1

### 5.3.2.3 Methanol and oil feed location

The feed location is one parameter that could affect the separation efficiency of hybridized RD. This section investigated the effect of methanol and CO feed location using WCO with 5%wt water content of 1 kmol/h, methanol 2 kmol/h, the total stage number of 26 and reflux ratio of 0.1. The effect of co-feed and separated feed was also studied to determine the optimum feed location.

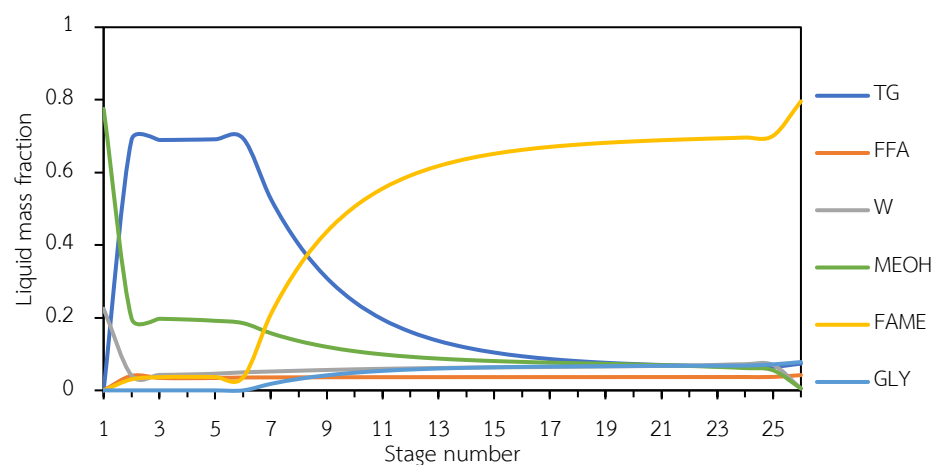


**Figure 5.17** Co-feed WCO and MEOH at stage 2

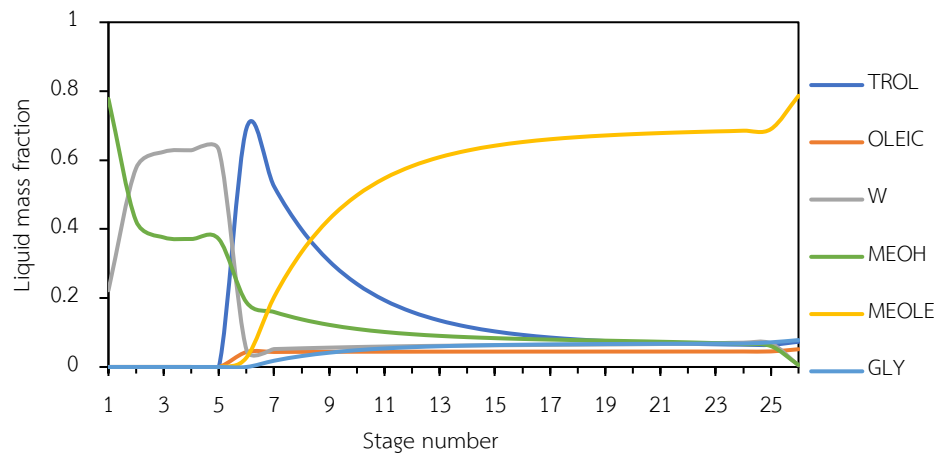


Figure 5.18 Co-feed WCO and MEOH at stage 6

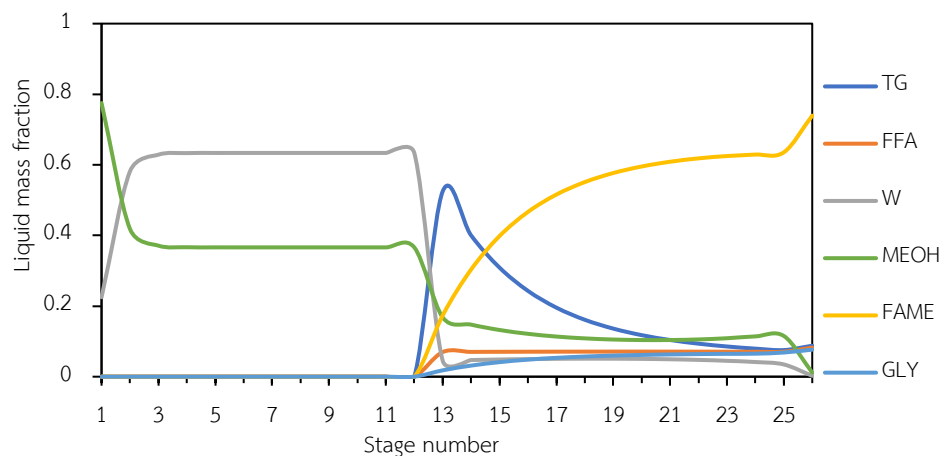


Figure 5.19 Co-feed WCO and MEOH at stage 13

Figures 5.17-5.18 present the co-feed of WCO with 5 %wt of water content at 2<sup>nd</sup>, 6<sup>th</sup> and 13<sup>th</sup> stage, respectively. It was found that for co-feed location of methanol and WCO at 2<sup>nd</sup> stage near the top of column, the methanol as the lightest phase was more likely to vaporize to the top of column leading to the presence of lower amount of methanol for transesterification section. The lower biodiesel yield was also obtained. When using co-feed location of methanol and WCO at 6<sup>th</sup> and 13<sup>th</sup>, the amount of FFA in WCO were still existed along the transesterification section even used co-feed location at 13<sup>th</sup> stage because FFA and WCO are large higher boiling than that of methanol resulting to flow down to the

bottom section without the presence of Amberlyst-15 as a catalyst to converted FFA. The present of FFA in the transesterification section might reduce the transesterification rate due to the lower concentration of reactant resulting to lower biodiesel yield and it purity.

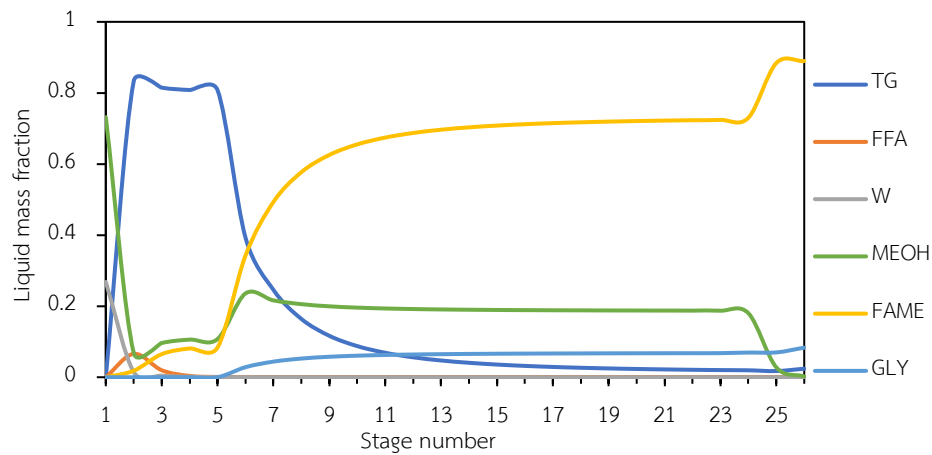


Figure 5.20 Feed WCO at stage 2 and MEOH at stage 6

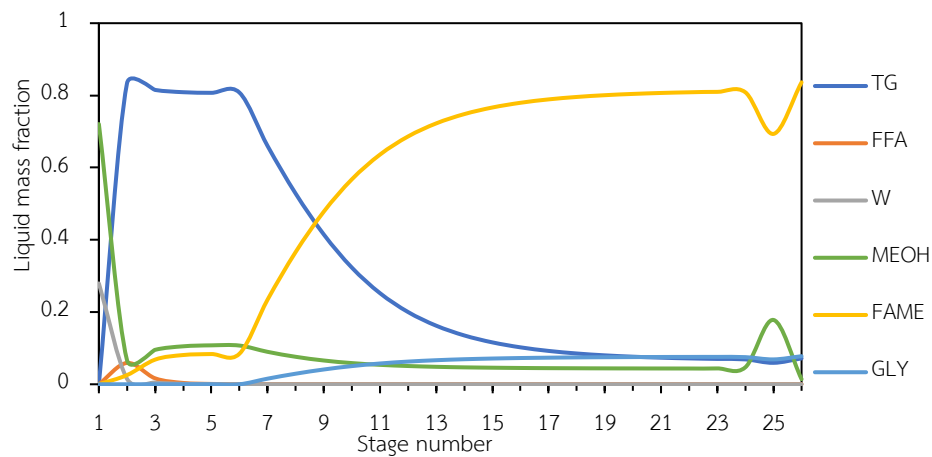


Figure 5.21 Feed WCO at stage 2 and MEOH at stage 25

Figures 5.20 and 5.21 illustrate the separated feed of WCO and methanol. WCO was fed at fixed location at 2<sup>nd</sup> stage while methanol was varied fed location at 6<sup>th</sup> and 25<sup>th</sup>. These results, in contrast to, co-feed location as WCO with FFA can flow down to the esterification section for converting of FFA resulting to higher biodiesel yield and purity than that of co-feed of methanol and WCO. However,

using the separated feed location of methanol at 25<sup>th</sup> stage provided the lower biodiesel yield and purity when compared to the separated feed location of methanol at 6<sup>th</sup> stage. This might be due to the fact that the methanol as a reactant for both esterification and transesterification was fed at 6<sup>th</sup> stage as the location between esterification and transesterification section resulting to provide the excess amount of methanol for both reactions. The highest biodiesel yield and purity were obtained at this separated feed location. Pérez-Cisneros et al. [12] also reported that the separated feed location of methanol and oil provided the highest triolein conversion for transesterification of 90-99.9% in the reactive distillation.





## Chapter 6

### Conclusions and recommendation

This section provided the conclusion and recommendation of this research as follows:

Kinetic model of Amberlyst-15 catalyzed esterification of decanoic acid using a Langmuir-Hinshelwood-Hougen-Watson (LHHW) approach can be used to predict Amberlyst-15 catalyzed esterification of oleic acid because there was no steric hindrance effect of oleic carbon atom compared to its decanoic acid.

The initial rate of transesterification was increased with increase of amount of water in WCO feedstocks in the range of 1 to 8 %wt. Water can promote the rate of transesterification because of the increase of active site as methoxide ion. However, the presence of water only 1%wt, the FAME concentration was remarkably reduced after reaching the maximum value because the saponification as a side reaction took place and the emulsion phase of water and oil was also performed.

The empirical kinetic model for transesterification of triolein in absence of water was proposed because of the trace amount of water was flown down to the transesterification section in the hybridize RD as found in the preliminary simulation results. The pseudo second-order of TG was fitted the experimental results with including of  $k_0$  and  $E_a$  determined from Arrhenius plot were equal to 15 and 36 kJ/mol, respectively.

Finally, the effect of water content on the ester-transesterification of hybridized RD performance was simulated using LHHW for esterification and pseudo-second for transesterification. The simulation of hybridized RD which can produce biodiesel according to standard EN 14214 was found to use 26 total stages including of 4 stages for esterification, 20 stages for transesterification with each rectifying and stripping stages. The optimum condition was using molar reflux ratio of 0.1 and

reboiler duty of 50-128 kW depending on water content (0-8 %wt). The suitable feed location should be separated between WCO and methanol using WCO feed location at top of column and methanol feed location at middle of column (first stage of transesterification).

### Recommendation

1. The presence of water can enhance the initial transesterification rate as well as reduce the induction period but lower the final biodiesel yield because of the presence of saponification. Therefore, the pretreatment to activated CaO catalyst and its stability should be also studied.
2. The hybridized RD using CaO catalyzed transesterification experimental set up should require longer period to reach steady state operation due to the presence of induction period. However, when the CaO catalyst is activated, the higher biodiesel yield should be achieved in a short startup time for hybridized RD. This hypothesis should be further investigated.
3. The presence of water does not only give rise the initial transesterification rate but also the saponification as a side reaction. Therefore, the optimum residence time in the hybridized RD should be further studied.

## REFERENCES



จุฬาลงกรณ์มหาวิทยาลัย  
**CHULALONGKORN UNIVERSITY**

## REFERENCES

- [1] Javidialesaadi, A. and Raeissi, S. Biodiesel production from high free fatty acid-content oils: experimental investigation of the pretreatment step. APCBEE Procedia 5 (2013): 474-478.
- [2] Gan, S., Ng, H.K., Chan, P.H., and Leong, F.L. Heterogeneous free fatty acids esterification in waste cooking oil using ion-exchange resins. Fuel Processing Technology 102 (2012): 67-72.
- [3] Son, S.M. and Kusakabe, K. Transesterification of sunflower oil in a countercurrent trickle-bed reactor packed with a CaO catalyst. Chemical Engineering and Processing: Process Intensification 50(7) (2011): 650-654.
- [4] Li, Z.-H., Lin, P.-H., Wu, J.C.S., Huang, Y.-T., Lin, K.-S., and Wu, K.C.W. A stirring packed-bed reactor to enhance the esterification–transesterification in biodiesel production by lowering mass-transfer resistance. Chemical Engineering Journal 234 (2013): 9-15.
- [5] Sundmacher, K. and Kienle, A. Reactive distillation: status and future directions. John Wiley & Sons, 2006.
- [6] Borugadda, V.B. and Goud, V.V. Biodiesel production from renewable feedstocks: status and opportunities. Renewable and Sustainable Energy Reviews 16(7) (2012): 4763-4784.
- [7] Vujicic, D., Comic, D., Zarubica, A., Micic, R., and Boskovic, G. Kinetics of biodiesel synthesis from sunflower oil over CaO heterogeneous catalyst. Fuel 89(8) (2010): 2054-2061.
- [8] Steinigeweg, S. and Gmehling, J. Esterification of a fatty acid by reactive distillation. Industrial & Engineering Chemistry Research 42(15) (2003): 3612-3619.
- [9] Shinde, G., Sapkal, V., Sapkal, R., and Raut, N. Transesterification by reactive distillation for synthesis and characterization of biodiesel. in Biodiesel- Feedstocks and Processing Technologies: InTech, 2011.
- [10] Boon-anuwat, N.-n., Kiatkittipong, W., Aiouache, F., and Assabumrungrat, S. Process design of continuous biodiesel production by reactive distillation:

- comparison between homogeneous and heterogeneous catalysts. Chemical Engineering and Processing: Process Intensification 92 (2015): 33-44.
- [11] Noshadi, I., Amin, N., and Parnas, R.S. Continuous production of biodiesel from waste cooking oil in a reactive distillation column catalyzed by solid heteropolyacid: optimization using response surface methodology (RSM). Fuel 94 (2012): 156-164.
- [12] Pérez-Cisneros, E.S., Mena-Espino, X., Rodríguez-López, V., Sales-Cruz, M., Viveros-García, T., and Lobo-Oehmichen, R. An integrated reactive distillation process for biodiesel production. Computers & Chemical Engineering 91 (2016): 233-246.
- [13] Petchsoongsakul, N., Ngaosuwan, K., Kiatkittipong, W., Aiouache, F., and Assabumrungrat, S. Process design of biodiesel production: Hybridization of ester-and transesterification in a single reactive distillation. Energy Conversion and Management 153 (2017): 493-503.
- [14] Liu, X., He, H., Wang, Y., Zhu, S., and Piao, X. Transesterification of soybean oil to biodiesel using CaO as a solid base catalyst. Fuel 87(2) (2008): 216-221.
- [15] 4 - Biodiesel Production. in Knothe, G., Krahl, J., and Van Gerpen, J. (eds.), The Biodiesel Handbook (Second Edition), pp. 31-96: AOCS Press, 2010.
- [16] Agarwal, A.K. Biofuels (alcohols and biodiesel) applications as fuels for internal combustion engines. Progress in Energy and Combustion Science 33(3) (2007): 233-271.
- [17] Knothe, G., Krahl, J., and Van Gerpen, J. The biodiesel handbook. Elsevier, 2015.
- [18] Verma, P. and Sharma, M.P. Review of process parameters for biodiesel production from different feedstocks. Renewable and Sustainable Energy Reviews 62 (2016): 1063-1071.
- [19] Talebian-Kiakalaieh, A., Amin, N.A.S., and Mazaheri, H. A review on novel processes of biodiesel production from waste cooking oil. Applied Energy 104 (2013): 683-710.

- [20] Tasić, M.B., Stamenković, O.S., and Veljković, V.B. Cost analysis of simulated base-catalyzed biodiesel production processes. Energy Conversion and Management 84 (2014): 405-413.
- [21] Boz, N., Degirmenbasi, N., and Kalyon, D.M. Esterification and transesterification of waste cooking oil over Amberlyst 15 and modified Amberlyst 15 catalysts. Applied Catalysis B: Environmental 165 (2015): 723-730.
- [22] Meher, L.C., Kulkarni, M.G., Dalai, A.K., and Naik, S.N. Transesterification of karanja (*Pongamia pinnata*) oil by solid basic catalysts. European Journal of Lipid Science and Technology 108(5) (2006): 389-397.
- [23] Li, Y., Lian, S., Tong, D., Song, R., Yang, W., Fan, Y., Qing, R., and Hu, C. One-step production of biodiesel from *Nannochloropsis* sp. on solid base Mg-Zr catalyst. Applied Energy 88(10) (2011): 3313-3317.
- [24] Shu, Q., Yang, B., Yuan, H., Qing, S., and Zhu, G. Synthesis of biodiesel from soybean oil and methanol catalyzed by zeolite beta modified with La<sup>3+</sup>. Catalysis Communications 8(12) (2007): 2159-2165.
- [25] Xie, W. and Li, H. Alumina-supported potassium iodide as a heterogeneous catalyst for biodiesel production from soybean oil. Journal of Molecular Catalysis A: Chemical 255(1-2) (2006): 1-9.
- [26] Pasupulety, N., Gunda, K., Liu, Y., Rempel, G.L., and Ng, F.T. Production of biodiesel from soybean oil on CaO/Al<sub>2</sub>O<sub>3</sub> solid base catalysts. Applied Catalysis A: General 452 (2013): 189-202.
- [27] Fogler, H.S. *Elements of chemical reaction engineering*. (1999).
- [28] Balat, M. and Balat, H. Progress in biodiesel processing. Applied Energy 87(6) (2010): 1815-1835.
- [29] Özbay, N., Oktar, N., and Tapan, N.A. Esterification of free fatty acids in waste cooking oils (WCO): Role of ion-exchange resins. Fuel 87(10-11) (2008): 1789-1798.
- [30] Connors, K.A. Chemical Kinetics: The Study of Reaction Rates in Solution. VCH, 1990.

- [31] Mazubert, A., Poux, M., and Aubin, J. Intensified processes for FAME production from waste cooking oil: a technological review. Chemical Engineering Journal 233 (2013): 201-223.
- [32] Cai, Z.-Z., Wang, Y., Teng, Y.-L., Chong, K.-M., Wang, J.-W., Zhang, J.-W., and Yang, D.-P. A two-step biodiesel production process from waste cooking oil via recycling crude glycerol esterification catalyzed by alkali catalyst. Fuel Processing Technology 137 (2015): 186-193.
- [33] Rehfinger, A. and Hoffmann, U. Kinetics of methyl tertiary butyl ether liquid phase synthesis catalyzed by ion exchange resin—I. Intrinsic rate expression in liquid phase activities. Chemical Engineering Science 45(6) (1990): 1605-1617.
- [34] Abd Rabu, R., Janajreh, I., and Honnery, D. Transesterification of waste cooking oil: Process optimization and conversion rate evaluation. Energy Conversion and Management 65 (2013): 764-769.
- [35] Deshmane, V.G. and Adewuyi, Y.G. Synthesis and kinetics of biodiesel formation via calcium methoxide base catalyzed transesterification reaction in the absence and presence of ultrasound. Fuel 107 (2013): 474-482.
- [36] Ye, W., Gao, Y., Ding, H., Liu, M., Liu, S., Han, X., and Qi, J. Kinetics of transesterification of palm oil under conventional heating and microwave irradiation, using CaO as heterogeneous catalyst. Fuel 180 (2016): 574-579.
- [37] Simasatitkul, L., Siricharnsakunchai, P., Patcharavorachot, Y., Assabumrungrat, S., and Arpornwichanop, A. Reactive distillation for biodiesel production from soybean oil. Korean Journal of Chemical Engineering 28(3) (2011): 649-655.
- [38] Chen, G.-Y., Shan, R., Yan, B.-B., Shi, J.-F., Li, S.-Y., and Liu, C.-Y. Remarkably enhancing the biodiesel yield from palm oil upon abalone shell-derived CaO catalysts treated by ethanol. Fuel Processing Technology 143 (2016): 110-117.
- [39] Das, K., Sahoo, P., Sai Baba, M., Murali, N., and Swaminathan, P.J.I.J.o.C.K. Kinetic studies on saponification of ethyl acetate using an innovative conductivity-monitoring instrument with a pulsating sensor. 43(11) (2011): 648-656.
- [40] Price, C.C. and Michel, R.H.J.J.o.t.A.C.S. Rates of Saponification of Substituted Ethyl 2-Naphthoates1. 74(14) (1952): 3652-3657.

- [41] Eze, V., Harvey, A., and Phan, A. Determination of the kinetics of biodiesel saponification in alcoholic hydroxide solutions. Vol. 140, 2015.
- [42] Theodorou, V., Skobridis, K., Tzakos, A.G., and Ragoussis, V.J.T.L. A simple method for the alkaline hydrolysis of esters. 48(46) (2007): 8230-8233.
- [43] Mata-Segreda, J.F.J.J.o.t.A.C.S. Hydroxide as general base in the saponification of ethyl acetate. 124(10) (2002): 2259-2262.
- [44] Kusmiyati, K. and Sugiharto, A. Production of biodiesel from oleic acid and methanol by reactive distillation. Bulletin of Chemical Reaction Engineering & Catalysis 5(1) (2010): 1-6.
- [45] Hadiyanto, H., Lestari, S.P., Abdullah, A., Widayat, W., Sutanto, H.J.I.J.o.E., and Engineering, E. The development of fly ash-supported CaO derived from mollusk shell of *Anadara granosa* and *Paphia undulata* as heterogeneous CaO catalyst in biodiesel synthesis. 7(3) (2016): 297-305.
- [46] Banchemo, M. and Gozzelino, G. A Simple Pseudo-Homogeneous Reversible Kinetic Model for the Esterification of Different Fatty Acids with Methanol in the Presence of Amberlyst-15. Vol. 11, 2018.
- [47] Banchemo, M. and Gozzelino, G. Nb2O5-catalyzed kinetics of fatty acids esterification for reactive distillation process simulation. Chemical Engineering Research and Design 100 (2015): 292-301.
- [48] Kouzu, M., Kasuno, T., Tajika, M., Sugimoto, Y., Yamanaka, S., and Hidaka, J. Calcium oxide as a solid base catalyst for transesterification of soybean oil and its application to biodiesel production. Fuel 87(12) (2008): 2798-2806.
- [49] Veljković, V.B., Stamenković, O.S., Todorović, Z.B., Lazić, M.L., and Skala, D.U. Kinetics of sunflower oil methanolysis catalyzed by calcium oxide. Fuel 88(9) (2009): 1554-1562.

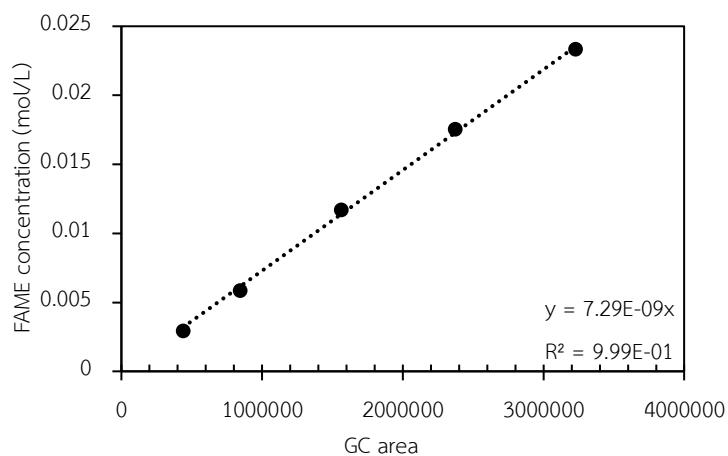


## Appendix A

Calibration curves for determining kinetic of esterification and transesterification

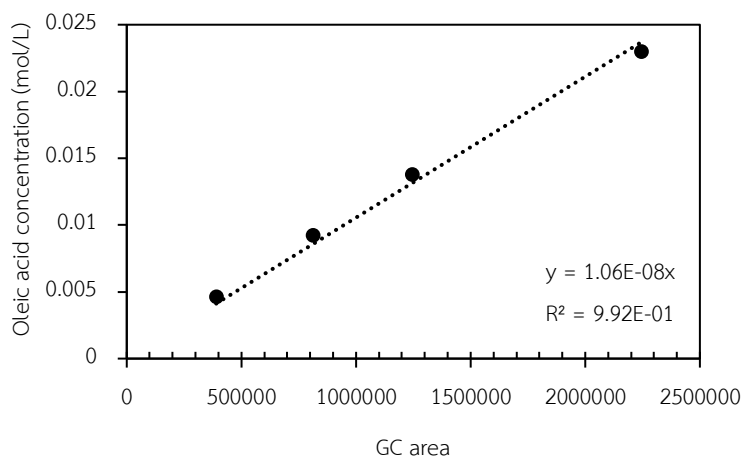
Standard curve of methyl oleate (FAME)

Plot between concentration of methyl oleate (FAME) in mol/L and GC area



Standard curve of oleic acid

Plot between concentration of oleic acid (FFA) in mol/L and GC area



## Appendix B

### Calculations of conversion and yield for esterification and transesterification

#### Esterification

The weight fraction is calculated by the following Eq B.1.

$$\text{Weight fraction} = \frac{C_{t,i} \times MW \times V_{t,0}}{\text{Mass}_{t,0}} \quad (\text{B.1})$$

where  $C_{t,i}$  is concentration of oleic acid at a difference time, MW is molecular weight of oleic acid,  $V_{t,0}$  is initial reaction volume of resulting sample and  $\text{Mass}_{t,0}$  is initial total mass of reaction mixture.

#### Transesterification

The biodiesel yield is calculated by the following Eq B.2.

$$\text{Biodiesel yield} = \frac{\text{FAME}_{t,i}}{\text{TG}_{t,0}} \times 100 \quad (\text{B.2})$$

where  $\text{FAME}_{t,i}$  is concentration of methyl oleate at different time and  $\text{TG}_{t,0}$  is initial trioleate.

## Appendix C

### Verification of kinetic esterification

**Table C1** Comparison of results between experiment and calculation with %error

Time (min)	Experiment	Calculation	%Error
0	0.61	0.64	4.99
30	0.41	0.37	10.54
60	0.34	0.32	4.50
90	0.30	0.29	1.51
120	0.27	0.28	3.26
150	0.25	0.26	4.82
180	0.25	0.25	0.59
210	0.23	0.25	8.44
240	0.23	0.24	3.57
270	0.23	0.24	5.36
300	0.21	0.23	9.90
330	0.23	0.23	2.19
360	0.22	0.23	5.87
390	0.22	0.23	4.84
420	0.22	0.23	4.57
450	0.21	0.23	7.55
480	0.20	0.22	12.41

**Table C2** Comparison of results between experiment and simulation with %error

Reflux Ratio	Experiment	Simulation	%Error
0.5	36.65	31.39	14.35
1	32.64	29.84	8.57
2	26.58	22.75	14.41

## Appendix D

## Empirical kinetic model for transesterification of triolein in presence of water

## Initial rate and overall rate

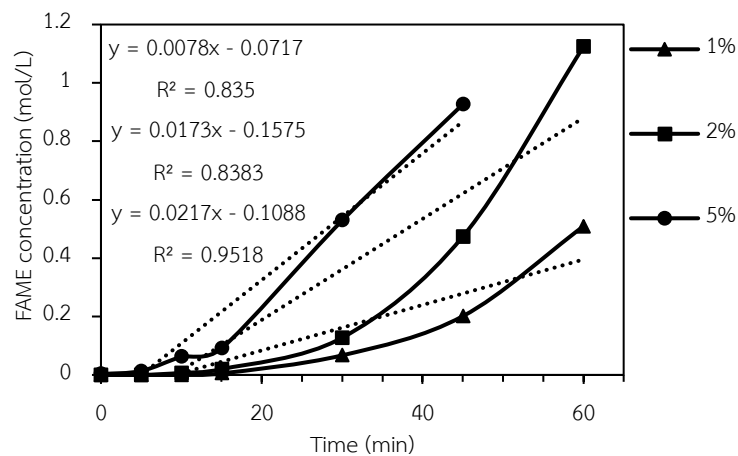


Figure D.1 Concentration of FAME profiles along the reaction time of initial experiment ( $\blacktriangle$  1%wt,  $\blacksquare$  2%wt and  $\bullet$  5%wt of water)

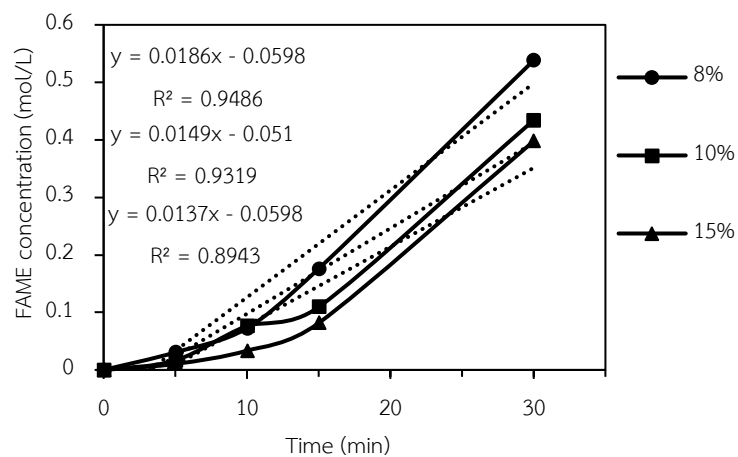



Figure D.2 Concentration of FAME profiles along the reaction time of initial experiment ( $\bullet$  8%wt,  $\blacksquare$  10%wt and  $\blacktriangle$  15%wt of water)

Table D.1 Results of overall rate reaction

Run	Initial rate (mol/g.min)	TG concentration (mol/L)	Methanol concentration (mol/L)	Water concentration (mol/L)
1	$1.95 \times 10^{-4}$	0.814	4.875	0.397
2	$2.73 \times 10^{-4}$	0.807	4.847	0.789
3	$3.57 \times 10^{-4}$	0.790	4.771	1.932
4	$2.28 \times 10^{-4}$	0.775	4.640	3.028
5	$2.12 \times 10^{-4}$	0.764	4.584	3.757
6	$2.36 \times 10^{-4}$	0.739	4.432	5.452
7	$4.21 \times 10^{-5}$	0.929	2.073	1.693
8	$6.56 \times 10^{-5}$	0.859	2.073	1.693
9	$4.54 \times 10^{-5}$	0.687	2.073	1.693
10	$4.64 \times 10^{-5}$	0.622	2.073	1.693
11	$2.47 \times 10^{-5}$	0.516	2.073	1.693
12	$1.80 \times 10^{-5}$	0.447	2.073	1.693
12	$2.48 \times 10^{-5}$	0.691	0.690	1.693
14	$9.57 \times 10^{-5}$	0.691	2.073	1.693
15	$2.06 \times 10^{-4}$	0.691	4.145	1.693
16	$2.35 \times 10^{-4}$	0.691	6.218	1.693

## Polymath regression

How to get Eq 5.1 from Program Polymath non-linear regression

1. Select regress and analyze data 
2. Put data from experiment result C01 is rate reaction, C02 is triglyceride concentration, C03 is methanol concentration and C04 is water concentration

POLYMATH 6.10 Educational Release - [Data Table]

File Program Edit Row Column Format Analysis Example

R015 : C008 C08 X ✓

	C01	C02	C03	C04	C05
01	4.21E-05	0.928992	2.072691	1.69311	
02	6.56E-05	0.859323	2.072691	1.69311	
03	4.54E-05	0.687458	2.072691	1.69311	
04	4.64E-05	0.621813	2.072691	1.69311	
05	2.47E-05	0.515594	2.072691	1.69311	
06	1.80E-05	0.446848	2.072691	1.69311	
07	2.48E-05	0.690889	0.690366	1.69311	
08	9.57E-05	0.690889	2.072691	1.69311	
09	2.06E-04	0.690889	4.145383	1.69311	
10	2.35E-04	0.690889	6.218074	1.69311	

3. Select nonlinear and put the model and initial guess

Regression Analysis Graph

Graph  Residuals

Report  Store Model

Linear & Polynomial | Multiple linear | Nonlinear

Model:

$C01=(A*(C02^w)*(C03^z))$

e.g.  $y = 2*x^A+B$

Model Parameters Initial Guess:

Model parm	Initial guess
A	1
w	1
z	1

4. Click 

5. Then get the report

**POLYMATH Report**  
Nonlinear Regression (L-M)

**Model:**  $C01 = (A*(C02^w)*(C03^z))$

Variable	Initial guess	Value	95% confidence
A	1.	2.934E-05	5.83E-06
w	1.	0.7976658	0.5242611
z	1.	1.345928	0.125258

**Nonlinear regression settings**  
Max # iterations = 64

**Precision**

R <sup>2</sup>	0.8606166
R <sup>2</sup> adj	0.8207928
Rmsd	8.681E-06
Variance	1.077E-09

**General**

Sample size	10
Model vars	3
Indep vars	2
Iterations	17

- First regression of TG and MeOH order

**Table D.2** First regression of TG and MeOH order

**Model:**  $C01 = A*(TG^w)*(MeOH^z)$

Variable	Initial guess	Value	95% confidence
A	1	2.93E-05	5.84E-06
w	1	0.797527	0.525291
z	1	1.345962	0.125504

**Precision**

R <sup>2</sup>	0.860174
R <sup>2</sup> adj	0.820224

The corresponding empirical rate is Eq C.1.

$$r_{tg} = 2.93 \times 10^{-5} [TG]^{0.79} [MeOH]^{1.34} \quad (D.1)$$

then regress data with w=0.5 and z=1 the result show in Table D.3

**Table D.3** Second regression of TG and MeOH order

Model: $C01 = A*(TG^{0.5})*(MeOH^1)$			
Variable	Initial guess	Value	95% confidence
A	1	4.27E-05	3.23E-09
Precision			
R <sup>2</sup>		0.799242	
R <sup>2</sup> adj		0.799242	

The corresponding empirical rate is Eq D.2.

$$r_{tg} = 4.27 \times 10^{-5} [TG]^{0.5} [MeOH] \quad (D.2)$$

After getting the order of TG and MeOH next determine empirical rate depend on concentration of water in form (Eq D.3).

$$r_{Fame} = \frac{C[H_2O]^x [TG]^{0.5} [MeOH]}{1 + d[H_2O]^y} \quad (D.3)$$

then use the Polymath regression program to find the parameter values C, x, d and y the result show in Table D.4

**Table D.4** First regression of water order

Model: $C01 = (c*(TG^{0.5})*MeOH*(H_2O^x))/(1+(d* H_2O ^y))$			
Variable	Initial guess	Value	95% confidence
c	0.1	0.045967	0.093681
x	0.1	0.66847	3.065261
d	0.1	0.097661	1.319493
y	0.1	2.58426	7.043031
Precision			
R <sup>2</sup>		0.9276446	
R <sup>2</sup> adj		0.7105784	



The corresponding empirical rate is Eq D.4.

$$r_{\text{Fame}} = \frac{0.046[\text{H}_2\text{O}]^{0.66}[\text{TG}]^{0.5}[\text{MeOH}]}{1+0.098[\text{H}_2\text{O}]^{2.58}} \quad (\text{D.4})$$

then regress data with x=0.5 and y=2.5 the result show in Table D.5

**Table D.5** Second regression of water order

Model: C01 = (c*(TG^0.5)*MeOH*(H <sub>2</sub> O^0.5))/(1+(d* H <sub>2</sub> O ^2.5))			
Variable	Initial guess	Value	95% confidence
c	1	4.58E-05	8.79E-08
d	1	0.016188	0.00015
<b>Precision</b>			
R <sup>2</sup>		0.712057	
R <sup>2</sup> adj		0.691489	

The corresponding empirical rate is Eq D.5.

$$r_{\text{Fame}} = \frac{4.58 \times 10^{-5} [\text{H}_2\text{O}]^{0.5} [\text{TG}]^{0.5} [\text{MeOH}]}{1+0.016[\text{H}_2\text{O}]^{2.5}} \quad (\text{D.5})$$

then try to regress data with y=1 because from Figure 5.4 trend of high water concentration show similar to low water concentration then the result show in Table D.6. R square and R square adjust higher than y=2.5

**Table D.6** Third regression of water order

Model: C01 = (c*(TG^0.5)*MeOH*(H <sub>2</sub> O^0.5))/(1+(d* H <sub>2</sub> O ^1))			
Variable	Initial guess	Value	95% confidence
c	1	7.78E-05	4.42E-05
d	1	0.464172	0.541116
<b>Nonlinear regression settings</b>			
Max # iterations = 64			
<b>Precision</b>			
R <sup>2</sup>		0.774419	
R <sup>2</sup> adj		0.758306	

Finally, we get Eq 5.1.

$$r_{\text{Fame}} = \frac{7.78 \times 10^{-5} [\text{H}_2\text{O}]^{0.5} [\text{TG}]^{0.5} [\text{MeOH}]}{1 + 0.46 [\text{H}_2\text{O}]} \quad (5.1)$$

### MatLab code

```

%%
%Input

%initial concentration
cTG = [0.812, 0.806, 0.789]; %Triglyceride
cMeOH = [4.9, 4.87, 4.77]; %Methanol
cFAME = 0; %Biodiesel
cGly = 0; %Glycerol
cH2O = [0.397, 0.789, 1.93]; %Water

%parameters
KEq = 0.9; %Equilibrium constant
Ea = 71871; %Ea (J/mol)
R = 8.314; %Gas constant (J/K.mol)
T = 333; %Temp (K)
k0 = 2.29e10; %k0

kT = k0*exp(-Ea/R/T); %New constant (T varied)

xp = zeros(501,3);

for i = 1:3
    k1 = kT*(cH2O(i)^0.5)/(1+50*cH2O(i));
    k2 = 0.003*(2*cH2O(i));

%%
%Integration

%Time
tspan = 0:1:500;

%initial & param
init = [cTG(i) cMeOH(i) cFAME cGly];
par = [k1 KEq k2];

[tt xx] = ode23s(@transes,tspan,init,[],par);

xp(:,i) = xx(:,3);
end

```

```

@transes
function dc = transes(t,c,par)

%Transesterification of triolein

%TG + 3MeOH <-> 3FAME + Gly
%2FAME + Ca(OH)2 -> Spon + 2MeOH

%%
%parameters
k1 = par(1);           %Forward 1st reaction constant
Keq1 = par(2);        %Equilibrium constant
k2 = par(3);          %Forward 2nd reaction constant

dc = zeros(4,1);

%%
%reaction
r1 = k1*(c(1)^0.5)*c(2);
r2 = (k1/Keq1)*c(3)*c(4);
r3 = k2*c(3)^1.5;

%%
dc(1,1) = -r1 + r2;   %triglyceride
dc(2,1) = -3*r1 + 3*r2 + 2*r3; %methanol
dc(3,1) = 3*r1 - 3*r2 - 2*r3;  %fame
dc(4,1) = r1 - r2;    %glycerol

end

```

Table D.8 result of Keq of difference %wt water

%wt Water	Keq
1	0.26
2	0.4
5	0.9

At 60°C temperature difference %wt water difference Keq because occur side reaction then the reaction is not at equilibrium, the result show in Table D.8

## Appendix E


## Empirical kinetic model for saponification

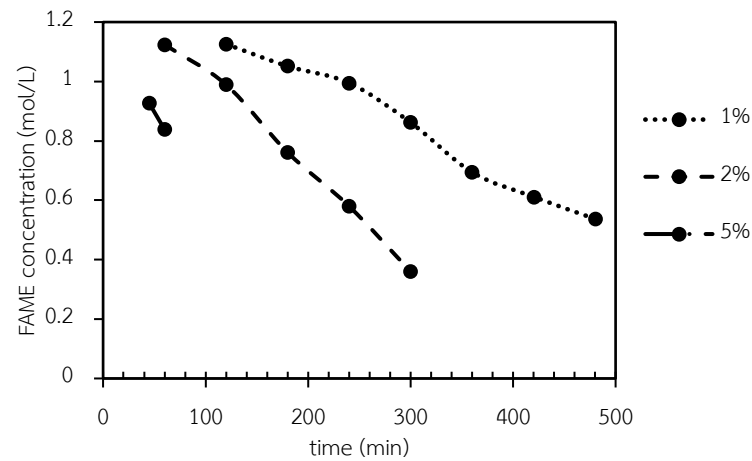


**Figure E.1** Result from experimental run 1-3, the concentration of FAME profile in saponification.

## Polymath regression

How to get kinetic model of saponification from Program Polymath non-linear regression

1. Select regress and analyze data 
2. Put data from experiment result C01 is rate reaction, C02 is FAME concentration and C03 is water concentration

POLYMATH 6.10 Educational Release - [Data Table]

File Program Edit Row Column Format Anal

R004 : C006 C06

	C01	C02	C03	C04
01	-5.5E-03	1.03175308	0.400600204	
02	-1.0E-02	1.045037297	0.789274448	
03	-1.8E-02	0.926693475	1.932046332	

3. Select nonlinear and put the model and initial guess

Regression | Analysis | Graph

Graph  Residuals

Report  Store Model

Linear & Polynomial | Multiple linear | Nonlinear

Model:  f(x)  L-M

$C01=k*(C02^x)*(2*C03^y)$

e.g.  $y = 2*x^A+B$

Model Parameters Initial Guess:

Model parm	Initial guess
k	1
x	1
y	1

4. Click →
5. Then get the report

**POLYMATH Report**  
Nonlinear Regression (L-M)

**Model:**  $C01 = k*(C02^x)*(2*C03^y)$

Variable	Initial guess	Value	95% confidence
k	1.	-0.005736	0
x	1.	1.469386	0
y	1.	0.8538505	0

**Nonlinear regression settings**  
Max # iterations = 64

**Precision**

R <sup>2</sup>	1.
R <sup>2</sup> adj	0
Rmsd	8.78E-16
Variance	1.0E+99

**General**

Sample size	3
Model vars	3
Indep vars	2
Iterations	6

- First regression of FAME and Water order

**Table D.2** First regression of FAME and Water order

Model: $C01 = k*(FAME^x)*(Water^y)$			
Variable	Initial guess	Value	95% confidence
k	1.	-0.005736	0
x	1.	1.469386	0
y	1.	0.8538505	0
Precision			
R <sup>2</sup>		1	
R <sup>2</sup> adj		0	

The corresponding empirical rate is Eq E.1.

$$r_{tg} = -0.005736[FAME]^{1.47}[MeOH]^{0.854} \quad (E.1)$$

then regress data with x=1.5 and y=1 the result show in Table D.5

**Table D.5** Second regression

Model: $C01 = k*(FAME^x)*(Water^y)$			
Variable	Initial guess	Value	95% confidence
k	1.	-0.005413	0.001124
Precision			
R <sup>2</sup>		0.9737307	
R <sup>2</sup> adj		0.9737307	

The corresponding empirical rate is Eq E.2.

$$r_{tg} = -0.005413[FAME]^{1.5}[MeOH] \quad (E.2)$$

## Appendix F

Empirical kinetic model for transesterification of triolein in absence of water

First order

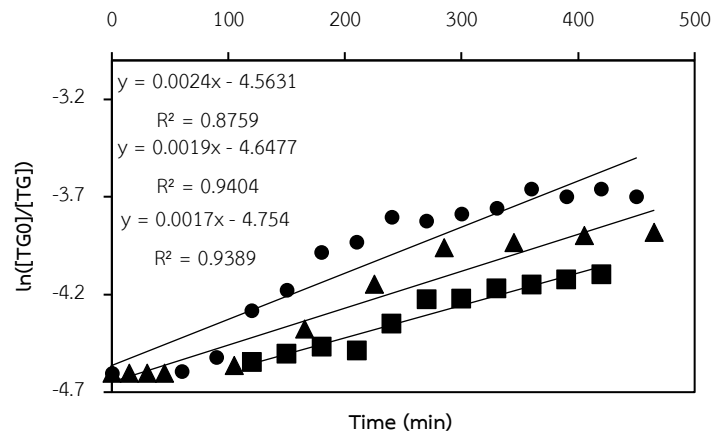


Figure F.1 Pseudo first-order reaction model of transesterification at various temperature 50-70°C.

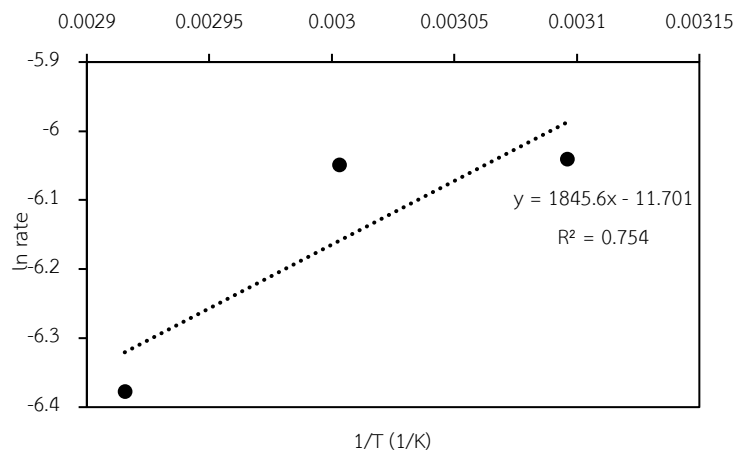
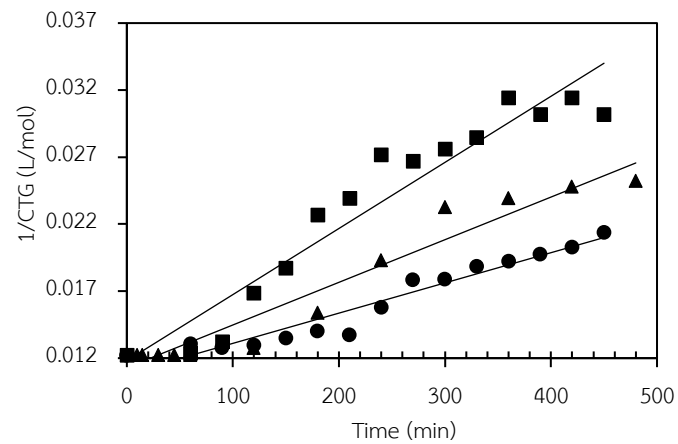
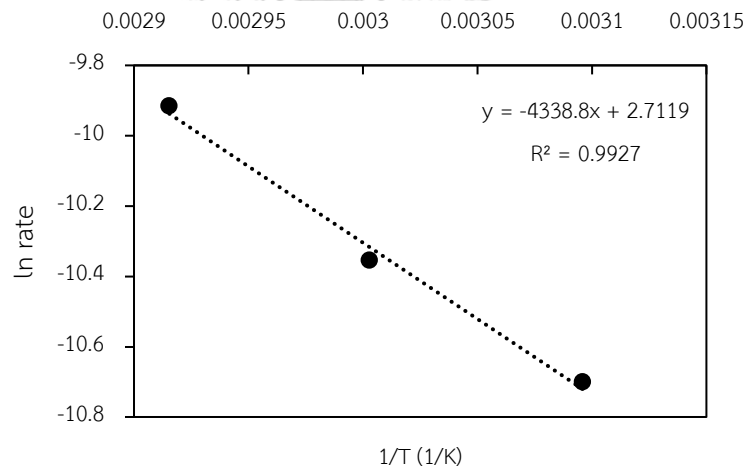


Figure F.2 Plot between  $\ln$  rate and  $1/T$  in Kelvin

## Second order



**Figure 5.7** Pseudo second-order reaction model of transesterification at various temperature 50-70°C.



**Figure 5.8** Plot between ln rate and 1/T in Kelvin

For pseudo first-order reaction result between ln rate and 1/T not fit show in Figure F.2 and result of pseudo second-order show fit data more than pseudo first-order



## Appendix G

## Hybridized RD in presence of water data

Condition are reflux ratio of 0.1 and reboiler duty 26.9 kW. Mass fraction of all components in each feed different residence time

**Table G.1** Residence time of 5 min

Mass Fractions	WCO	MEOH	BOT	DIS	FAME	GLY
TG	0.869565	0	2.57E-08	5.17E-15	2.57E-08	0
MEOH	0	1	1.24E-02	8.45E-01	1.24E-02	0
FAME	0	0	8.89E-01	2.42E-06	8.89E-01	0
GLY	0	0	8.36E-02	1.29E-22	8.36E-02	0
FFA	0.086957	0	3.10E-03	8.00E-07	3.10E-03	0
WATER	0.043478	0	1.21E-02	1.55E-01	1.21E-02	0
CAOLE	0	0	4.52E-06	2.11E-32	4.52E-06	0

**Table G.2** Residence time of 10 min

Mass Fractions	WCO	MEOH	BOT	DIS	FAME	GLY
TG	0.869565	0	2.57E-08	5.17E-15	2.57E-08	0
MEOH	0	1	1.24E-02	8.45E-01	1.24E-02	0
FAME	0	0	8.89E-01	2.42E-06	8.89E-01	0
GLY	0	0	8.36E-02	1.29E-22	8.36E-02	0
FFA	0.086957	0	3.10E-03	8.01E-07	3.10E-03	0
WATER	0.043478	0	1.21E-02	1.55E-01	1.21E-02	0
CAOLE	0	0	4.52E-06	0.00E+00	4.52E-06	0

**Table G.3** Residence time of 20 min

Mass Fractions	WCO	MEOH	BOT	DIS	FAME	GLY
TG	0.869565	0	2.57E-08	5.19E-15	2.57E-08	0
MEOH	0	1	1.25E-02	8.45E-01	1.25E-02	0
FAME	0	0	8.89E-01	2.63E-06	8.89E-01	0
GLY	0	0	8.36E-02	1.29E-22	8.36E-02	0
FFA	0.086957	0	3.04E-03	6.26E-07	3.04E-03	0
WATER	0.043478	0	1.21E-02	1.55E-01	1.21E-02	0
CAOLE	0	0	4.52E-06	1.83E-24	4.52E-06	0

**Table G.4** Residence time of 30 min

Mass Fractions	WCO	MEOH	BOT	DIS	FAME	GLY
TG	0.869565	0	2.57E-08	5.20E-15	2.57E-08	0
MEOH	0	1	1.25E-02	8.45E-01	1.25E-02	0
FAME	0	0	8.89E-01	2.70E-06	8.89E-01	0
GLY	0	0	8.36E-02	1.29E-22	8.36E-02	0
FFA	0.086957	0	3.02E-03	5.61E-07	3.02E-03	0
WATER	0.043478	0	1.20E-02	1.55E-01	1.20E-02	0
CAOLE	0	0	4.52E-06	7.27E-29	4.52E-06	0

## Appendix H

### Hybridized RD in absence of water data

Tables H.1-4 show mass fraction of different streams in RD from operation using WCO with different water contents for methanol to TG molar ratio of 7 to 1, reflux ratio of 0.1, stage residence time of 60 min and total stage number of 26 including 4 stages for esterification, 20 stages for transesterification, one rectifying and one stripping stages to produce biodiesel yield more than 96.5%.

**Table H.1** 1%wt Water in WCO

Mass Fractions	WCO	MEOH	BOT	DIS	FAME	GLY
TROL	0.900901	0	0.023865	2.64E-16	1.68E-09	0.025905
OLEIC	0.09009	0	1.21E-04	3.32E-08	1.43E-05	1.30E-04
MEOH	0	1	0.003141	0.895795	0.018106	0.001862
GLY	0	0	0.083179	1.84E-15	0.979146	0.006593
MEOLE	0	0	0.889694	8.39E-07	0.002734	0.96551
W	0.009009	0	2.15E-11	0.104205	9.79E-11	1.50E-11

**Table H.2** 2%wt Water in WCO

Mass Fractions	WCO	MEOH	BOT	DIS	FAME	GLY
TROL	0.892857	0	0.023942	1.66E-16	1.65E-09	0.025984
OLEIC	0.089286	0	3.33E-04	4.79E-08	3.93E-05	3.58E-04
MEOH	0	1	0.002715	0.830709	0.015682	0.001609
GLY	0	0	0.083209	3.63E-16	0.981575	0.006592
MEOLE	0	0	0.8898	4.55E-07	0.002704	0.965457
W	0.017857	0	4.76E-11	0.169291	2.16E-10	3.32E-11

**Table H.3** 5%wt Water in WCO

Mass Fractions	WCO	MEOH	BOT	DIS	FAME	GLY
TROL	0.869565	0	0.024009	7.25E-17	1.60E-09	0.02605
OLEIC	0.086957	0	8.86E-04	3.90E-08	1.04E-04	9.53E-04
MEOH	0	1	0.002172	0.731829	0.012569	0.001288
GLY	0	0	0.083252	1.02E-17	0.98466	0.006598
MEOLE	0	0	0.889681	1.22E-07	0.002667	0.965111
W	0.043478	0	8.69E-11	0.26817	3.95E-10	6.07E-11

**Table H.4** 8%wt Water in WCO

Mass Fractions	WCO	MEOH	BOT	DIS	FAME	GLY
TROL	0.847458	0	0.023763	6.09E-17	1.67E-09	0.025793
OLEIC	0.084746	0	1.18E-03	3.99E-08	1.39E-04	1.27E-03
MEOH	0	1	0.002998	0.655906	0.017275	0.001779
GLY	0	0	0.083206	6.77E-18	0.979863	0.00662
MEOLE	0	0	0.888856	6.66E-08	0.002723	0.964542
W	0.067797	0	1.95E-10	0.344094	8.88E-10	1.36E-10

Tables H.5 and H.6 show mass fraction of different streams in RD from operation using different number of transesterification stage for methanol to TG molar ratio of 7 to 1, reflux ratio of 0.1 and stage residence time of 60 min.

**Table H.5** 14 stages for transesterification

Mass Fractions	WCO	MEOH	BOT	DIS	FAME	GLY
TROL	0.869565	0	0.109133	7.07E-17	1.43E-08	0.11778
OLEIC	0.086957	0	3.20E-04	3.57E-08	4.43E-05	3.42E-04
MEOH	0	1	0.011413	0.731578	0.066951	0.007012
GLY	0	0	0.074396	3.53E-22	0.929737	0.006623
MEOLE	0	0	0.804738	1.53E-07	0.003268	0.868242
W	0.043478	0	2.84E-08	0.268422	1.37E-07	1.98E-08

**Table H.6** 18 stages for transesterification

Mass Fractions	WCO	MEOH	BOT	DIS	FAME	GLY
TROL	0.869565	0	0.079174	6.94E-17	8.14E-09	0.085612
OLEIC	0.086957	0	3.12E-04	3.33E-08	4.06E-05	3.34E-04
MEOH	0	1	0.008161	0.731574	0.047644	0.00495
GLY	0	0	0.077512	4.48E-22	0.949275	0.006614
MEOLE	0	0	0.834842	1.75E-07	0.003041	0.90249
W	0.043478	0	2.80E-09	0.268426	1.32E-08	1.95E-09

Tables H.7-10 show mass fraction of different streams in RD from operation using different feed location for methanol to TG molar ratio of 7 to 1, reflux ratio of 0.1, stage residence time 60 of min and total stage number of 26 including 4 stages for esterification, 20 stages for transesterification, one rectifying and one stripping stages.

**Table H.7** Co feed at stage 2

Mass Fractions	WCO	MEOH	BOT	DIS	FAME	GLY
TROL	0.869565	0	0.073646	5.24E-16	9.47E-09	0.079682
OLEIC	0.086957	0	4.21E-02	2.06E-08	5.87E-03	4.50E-02
MEOH	0	1	0.005347	0.775114	0.030354	0.003297
GLY	0	0	0.078022	2.71E-26	0.935623	0.007728
MEOLE	0	0	0.795897	3.06E-07	0.003341	0.86086
W	0.043478	0	5.04E-03	0.224886	2.48E-02	3.42E-03

**Table H.8** Co feed at stage 6

Mass Fractions	WCO	MEOH	BOT	DIS	FAME	GLY
TROL	0.869565	0	0.073277	7.63E-16	9.70E-09	0.079274
OLEIC	0.086957	0	5.15E-02	1.51E-08	7.12E-03	5.51E-02
MEOH	0	1	0.005763	0.777463	0.032318	0.00359
GLY	0	0	0.078084	1.85E-20	0.933871	0.008045
MEOLE	0	0	0.786597	3.41E-07	0.003327	0.850702
W	0.043478	0	4.78E-03	0.222537	2.34E-02	3.26E-03

**Table H.9** Co feed at stage 13

Mass Fractions	WCO	MEOH	BOT	DIS	FAME	GLY
TROL	0.869565	0	0.087699	3.14E-13	1.53E-08	0.09476
OLEIC	0.086957	0	8.24E-02	1.15E-07	1.13E-02	8.81E-02
MEOH	0	1	0.011491	0.774944	0.061235	0.007486
GLY	0	0	0.076559	6.35E-26	0.91258	0.009251
MEOLE	0	0	0.739432	2.56E-06	0.003411	0.79869
W	0.043478	0	2.44E-03	0.225054	1.15E-02	1.71E-03

**Table H.10** Separated feed of WCO at stage 2 and methanol at stage 25

Mass Fractions	WCO	MEOH	BOT	DIS	FAME	GLY
TROL	0.869565	0	0.071671	6.81E-17	1.04E-08	0.077734
OLEIC	0.086957	0	2.36E-04	3.42E-08	3.28E-05	2.54E-04
MEOH	0	1	0.014054	0.720646	0.0794	0.008526
GLY	0	0	0.077717	4.53E-20	0.917052	0.006718
MEOLE	0	0	0.836321	1.64E-07	0.003515	0.906768
W	0.043478	0	7.16E-22	0.279354	0.00E+00	0.00E+00

## VITA

**NAME** Ajala Anantapinitwatna

**DATE OF BIRTH** 22 November 1993

**PLACE OF BIRTH** Mahasarakham, Thailand

**INSTITUTIONS ATTENDED** Bachelor degree of Chemical engineering, Khon Kaen university, 2012-2016 A.D.  
Master's degree in Chemical engineering, Chulalongkorn university, 2016-2019 A.D.



จุฬาลงกรณ์มหาวิทยาลัย  
**CHULALONGKORN UNIVERSITY**